
Approximate discounting-free policy evaluation from transient and recurrent states

Vektor Dewanto, Marcus Gallagher

School of Information Technology and Electrical Engineering
University of Queensland, Australia
v.dewanto@uqconnect.edu.au, marcusg@uq.edu.au

Abstract

In order to distinguish policies that prescribe good from bad actions in transient states, we need to evaluate the so-called bias of a policy from transient states. However, we observe that most (if not all) works in approximate discounting-free policy evaluation thus far are developed for estimating the bias solely from recurrent states. We therefore propose a system of approximators for the bias (specifically, its relative value) from transient and recurrent states. Its key ingredient is a seminorm LSTD (least-squares temporal difference), for which we derive its minimizer expression that enables approximation by sampling required in model-free reinforcement learning. This seminorm LSTD also facilitates the formulation of a general unifying procedure for LSTD-based policy value approximators. Experimental results validate the effectiveness of our proposed method.

1 Introduction

Consider an environment where there are two types of states: those that are visited infinitely many times by an agent, and those that are not (even though the agent is modelled to operate up to infinity). The members of the former group are called recurrent states, whereas those of the latter are called transient states. If all recurrent states form a single closed irreducible set, then we have the so-called unichain Markov chain (MC). It is closed in that once the agent is in any member of the set, the agent cannot go outside to any non-member state. It is irreducible because from any member of the set, the agent can visit any other member. In reinforcement learning (RL), such a unichain MC is induced by (at least) one of the stationary policies of the Markov decision process (MDP) model, for which we call such a model a unichain MDP.

The work in this paper is concerned with evaluating a stationary policy π from both transient and recurrent states in terms of discounting-free evaluation functions. Particularly, the policy value function of interest is the bias (denoted by v_b) of π as follows,

$$v_b(\pi, s) := \lim_{t_{\max} \rightarrow \infty} \mathbb{E}_{A_t \sim \pi(\cdot|s_t), S_{t+1} \sim p(\cdot|s_t, a_t)} \left[\sum_{t=0}^{t_{\max}-1} \left(r(S_t, A_t) - v_g(\pi) \right) \middle| S_0 = s, \pi \right], \quad \forall s \in \mathcal{S}, \quad (1)$$

where S_t and A_t are discrete state and action random variables on the state set \mathcal{S} and action set \mathcal{A} of an infinite-horizon MDP with one-step state transition distribution p , and reward function r . Here, v_g denotes the gain (the average-reward) value function, which is state-invariant whenever the induced MC is unichain. Both bias and gain do not involve any discount factor (hence, they are said to be discounting-free; cf. the discounted reward value function).

Evaluating the bias from both state types is essential for carrying out further policy selection on gain-optimal policies that induce unichain MCs. This is because the gain value function only concerns with the long-run rewards (which are earned in recurrent states). It ignores rewards earned at the

outset in transient states, in which gain-optimal policies therefore cannot distinguish “good” from “bad” actions. In other words, they are suboptimal in transient states with respect to the finest (the most selective) optimality criterion, i.e. the Blackwell optimality.

Despite the aforementioned importance, we observe that most works in RL are designed for approximately evaluating a policy from recurrent states, specifically for MDPs whose all induced MCs have only recurrent states. The stationary state distribution is used for weighting the state-wise error terms in the error function. This applies to both discounted and discounting-free policy evaluation, e.g. (Liu and Olshevsky, 2021, Assumption 3), (Dann et al., 2014, Sec 2.4.2). There are a few works that estimate the policy values from transient states. However, they are applicable merely for MCs with a single recurrent state whose reward is zero and known (thus no estimation is needed). For instance, Bradtke and Barto (1996, Thm 1) proposed a discounted-reward estimator for environments with multiple transient states and a single 0-reward absorbing terminal state. The error terms are weighted by the visitation probabilities of transient states from the initial time until absorption, which is known to happen at the last timestep of a trial (as the agent reaches the absorbing terminal state).

In this paper, we propose techniques that approximate the bias value (of any stationary policy) from multiple transient and recurrent states in model-free RL. This requires value approximation from both state types, instead of either one out of two types as the above-mentioned existing works. Moreover, the state classification is unknown since the agent does not know the state transition distribution and does not attempt to estimate it. This also implies that the agent does not know when it is absorbed into the closed, irreducible recurrent state set (i.e. the absorption time). If the state classification was known, the state set could be sliced and two approximators could be built: one for the recurrent states and one for the transient states; taking advantage of the existing works. However in that case, some additional work would still be needed for two reasons. First is that all recurrent states cannot simply be separated from the state set (for the sake of the transient state value approximator) because there must be transitions from some transient states to recurrent states, which may have non-zero rewards affecting transient state values. Second is because those two individual bias approximators have different offsets from the true bias (due to the nature of the error function that they minimize). Therefore, their approximation results need to be calibrated before being used simultaneously in a formula that involves bias values of both transient and recurrent states. More exposition about these two issues are provided later in Secs 3 and 5.

We present a system of approximators for the bias (relative) value. Each approximator is based on least-squares temporal difference (LSTD). In one extreme (where the computation cost is put aside), the system instantiates stepwise LSTD approximators that use stepwise state distributions, denoted as p_π^t , to weight the state-wise error terms. Here, $p_\pi^t(s) := \mathbb{E}_{S_0 \sim \hat{p}}[\Pr\{S_t = s | S_0, \pi\}]$, $\forall s \in \mathcal{S}$, which indicates the probability of visiting a state s in t timesteps when the agent begins at an initial state $S_0 \sim \hat{p}$ then follows a policy π . Such a system dismisses the need for state classification, but poses at least three challenges, for which we contribute some solutions.

First, the stepwise state distribution p_π^t may not have the whole state set as its support. For example, when the agent can only begin in transient states, $p_\pi^{t=0}$ has zero probability for any recurrent state. The same goes for transient states with respect to p_π^t after the stationary state distribution is reached (as there is no chance of visiting transient states once the recurrent class is entered). Consequently, the diagonal matrix derived from p_π^t may be positive semidefinite (PSD). This necessitates an LSTD approximator that involves a seminorm, hence a generalized pseudoinverse. The main difficulty comes from the fact that the reverse product law does not apply to pseudoinverse. We derive the optimal (minimizing) parameter of the seminorm LSTD, and its sampling-based estimator in Sec 3.

Second, a system of *stepwise* approximators requires at least one parameter per timestep. This implies an infinite number of parameters whenever there is an infinite number of timesteps (as in infinite-horizon MDPs). To be practical, we propose a procedure that accommodates the specification of the desired number of approximators (hence, the desired number of parameters in a system). It determines a number of timestep neighborhoods according to sampling-based estimated distances among stepwise state distributions. For every neighborhood, it then applies a seminorm LSTD that weights the state-wise error terms using the average state distributions on that neighborhood. This procedure is general and unifies existing LSTD-based methods, as explained in Sec 4.

Third, the approximators of the proposed system estimate the bias only up to some offset; generally one unique offset for each approximator. This is inherently due to the limitation of the bias error-function that those approximators individually minimize. In order to use the resulting approximations

(of all approximators) in a formula that jointly involves transient and recurrent state values, we need to calibrate those offsets so that all approximations have one common offset with respect to the true bias, which is time-invariant. In Sec 5, we describe such offset calibration along with the pseudocode of the proposed system of seminorm LSTD approximators for the bias (i.e. its relative value).

We provide experimental results in Sec 7, which is preceded by experimental setup in Sec 6. Finally, we conclude this work in Sec 8, where we also describe its limitations as well as some avenues for future research. The next Sec 2 presents some necessary prerequisites for this work.

2 Preliminaries

Given a stationary policy π , we are interested in computing its bias value $v_b(\pi, s), \forall s \in \mathcal{S}$ as in (1). Since the policy and the value function type are fixed, we often simplify their notations and write $v(s) := v_b(\pi, s)$. This $v(s)$ is then called a state value of s .

A parametric state-value approximator is parameterized by a parameter vector $\mathbf{w} \in \mathcal{W} = \mathbb{R}^{\dim(\mathbf{w})}$. Linear parameterization (which is the focus of this work) gives

$$\hat{v}(s, \mathbf{w}) := \mathbf{w}^\top \cdot \mathbf{f}(s) \approx v(s), \quad \forall s \in \mathcal{S}, \forall \mathbf{w} \in \mathcal{W}, \quad \text{equivalently,} \quad \hat{\mathbf{v}}(\mathbf{w}) = \mathbf{F}\mathbf{w}, \quad (2)$$

where $v(s)$ denotes the true (ground-truth) state value of s , $\mathbf{f}(s) \in \mathbb{R}^{\dim(\mathbf{w})}$ the state feature vector of s , and $\mathbf{F} \in \mathbb{R}^{|\mathcal{S}| \times \dim(\mathbf{w})}$ the corresponding state feature matrix (whose s -th row contains $\mathbf{f}^\top(s)$). Here, the approximate state value vector $\hat{\mathbf{v}} \in \mathbb{R}^{|\mathcal{S}|}$ is obtained by stacking all scalar approximations $\hat{v}(s) \in \mathbb{R}, \forall s \in \mathcal{S}$ on top of each other.

One way to learn \mathbf{w} is by minimizing the weighted mean squared projected Bellman error (MSPBE), denoted as $\tilde{e}_{\mathbb{P}\mathbb{B}}(\mathbf{w})$ in (4). This error function is derived based on the identity in the average-reward Bellman equation, namely

$$v(s_t) = r(s_t) - g + \mathbb{E}_{p(\cdot|s_t)}[v(S_{t+1})], \quad \forall s_t \in \mathcal{S}, \quad \text{equivalently,} \quad \mathbf{v} = \mathbf{r} - \mathbf{g} + \mathbf{P}\mathbf{v} =: \mathbb{B}[\mathbf{v}], \quad (3)$$

and some projection to obtain the representation of $\mathbb{B}[\mathbf{v}]$ in the parameter space. Here, the reward function $r(s_t) = \mathbb{E}_\pi[r(s_t, A_t)]$ corresponds to the reward vector $\mathbf{r} \in \mathbb{R}^{|\mathcal{S}|}$, the gain $g := v_g(\pi)$ corresponds to the gain vector $\mathbf{g} := g\mathbf{1} \in \mathbb{R}^{|\mathcal{S}|}$ (using the vector $\mathbf{1}$, whose entries are all 1's), and $\mathbf{P} \in \mathbb{R}^{|\mathcal{S}| \times |\mathcal{S}|}$ is the one-step state transition stochastic matrix of an induced MC, whose s_t -th row represents a next-state conditional distribution $p_\pi(S_{t+1}|s_t) = \sum_{a_t \in \mathcal{A}} \pi(a_t|s_t)p(S_{t+1}|s_t, a_t)$. The operator $\mathbb{B} : \mathbb{R}^{|\mathcal{S}|} \mapsto \mathbb{R}^{|\mathcal{S}|}$ is termed as the Bellman policy-evaluation operator on $\mathbf{v} \in \mathbb{R}^{|\mathcal{S}|}$.

The MSPBE is defined as follows,

$$\tilde{e}_{\mathbb{P}\mathbb{B}}(\mathbf{w}) := \underbrace{\|\hat{\mathbf{v}}(\mathbf{w}) - \tilde{\mathbb{P}}\mathbb{B}\hat{\mathbf{v}}(\mathbf{w})\|_{\tilde{\mathbf{p}}}}_{\Delta_{\hat{\mathbf{v}}}}^2 = \Delta_{\hat{\mathbf{v}}}^\top \mathbf{D}_{\tilde{\mathbf{p}}} \Delta_{\hat{\mathbf{v}}} = \sum_{s \in \mathcal{S}} \tilde{p}(s) \Delta_{\hat{v}[s]}^2, \quad (4)$$

where $\tilde{\mathbf{p}} \in \mathbb{R}^{|\mathcal{S}|}$ is a vector of probability values of some state distribution $\tilde{p}(s) = \Pr\{S = s\}, \forall s \in \mathcal{S}$, and $\mathbf{D}_{\tilde{\mathbf{p}}}$ is an $|\mathcal{S}|$ -by- $|\mathcal{S}|$ diagonal matrix with $\tilde{\mathbf{p}}$ along its diagonal. Here, $\tilde{\mathbb{P}}$ denotes a projection operator such that

$$\tilde{\mathbb{P}}\mathbf{v} = \mathbf{F}\mathbf{w}^\diamond, \quad \text{where } \mathbf{w}^\diamond = \underset{\mathbf{w} \in \mathcal{W}}{\operatorname{argmin}} \left\{ \|\mathbf{F}\mathbf{w} - \mathbf{v}\|_{\tilde{\mathbf{p}}}^2 = \sum_{s \in \mathcal{S}} \tilde{p}(s) (\mathbf{f}^\top(s) \mathbf{w} - v(s))^2 \right\}. \quad (5)$$

At this stage, what is left to fully define $\tilde{e}_{\mathbb{P}\mathbb{B}}$ is the state distribution \tilde{p} , whose probability values serve as weights in (4) and (5). For recurrent MCs, one natural choice for \tilde{p} is the stationary state distribution p^* that indicates the state visitation frequency in the long-run. More precisely,

$$p^*(s) = \mathbb{E}_{S_0 \sim \tilde{p}} \left[p^*(s|s_0) := \lim_{t_{\max} \rightarrow \infty} \frac{1}{t_{\max}} \sum_{t=0}^{t_{\max}-1} p^t(s|s_0) = \underbrace{\lim_{t_{\max} \rightarrow \infty} p^{t_{\max}}(s|s_0)}_{\text{when the MC is aperiodic}} \right], \quad \forall s \in \mathcal{S}, \quad (6)$$

where $p^*(s|s_0)$ is the limiting distribution of the stepwise $p^t(s|s_0)$ as t goes to infinity (nonetheless, p^* may be achieved in finite time). Since all states of a recurrent MC are recurrent, its p^* has the whole state set as its support, i.e. $p^*(s) > 0, \forall s \in \mathcal{S}$. This is advantageous because \mathbf{D}_{p^*} is positive definite (PD) so that (4) and (5) involve a (weighted Euclidean) norm, and the inverse $\mathbf{D}_{p^*}^{-1}$ exists.

Assumption 2.1. *The state feature matrix \mathbf{F} has a full column rank. This is equivalent to saying that all state feature vectors are linearly independent.* (Remark: this assumption is not required by our proposed seminorm LSTD in Sec 3.)

In fact, setting $\tilde{\mathbf{p}} \leftarrow \mathbf{p}^*$ leads to the LSTD method for recurrent MDPs (Yu and Bertsekas, 2009). Whenever Assumption 2.1 is satisfied, the projection operator in (4) is defined as $\mathbb{P} := \mathbf{F}(\mathbf{F}^\top \mathbf{D}_{\tilde{\mathbf{p}}} \mathbf{F})^{-1} \mathbf{F}^\top \mathbf{D}_{\tilde{\mathbf{p}}}$. Then, the optimal parameter value (which minimizes $\tilde{e}_{\mathbb{P}\mathbb{B}}$) is given by

$$\mathbf{w}^* = \mathbf{X}^{-1} \mathbf{y}, \quad \text{where } \mathbf{w}^* \in \mathcal{W} \text{ and} \quad (7)$$

$$\begin{aligned} \mathbf{X} &= \sum_{s \in \mathcal{S}} p^*(s) \sum_{s' \in \mathcal{S}} p(s'|s) \left[\mathbf{f}(s) \left(\mathbf{f}(s) - \mathbf{f}(s') \right)^\top \right] = \sum_{s \in \mathcal{S}} p^*(s) \mathbf{f}(s) \left[\left(\mathbf{f}(s) - \sum_{s' \in \mathcal{S}} p(s'|s) \mathbf{f}(s') \right)^\top \right] \\ &= \mathbf{F}^\top \mathbf{D}_{\tilde{\mathbf{p}}} (\mathbf{I} - \mathbf{P}) \mathbf{F} \quad \in \mathbb{R}^{\dim(\mathbf{w}) \times \dim(\mathbf{w})}, \text{ with an identity matrix } \mathbf{I} \in \mathbb{R}^{|\mathcal{S}| \times |\mathcal{S}|}, \text{ and} \end{aligned} \quad (8)$$

$$\begin{aligned} \mathbf{y} &= \sum_{s \in \mathcal{S}} p^*(s) \sum_{a \in \mathcal{A}} \pi(a|s) \left[(r(s, a) - g) \mathbf{f}(s) \right] = \sum_{s \in \mathcal{S}} p^*(s) \left[(r(s) - g) \mathbf{f}(s) \right] \\ &= \mathbf{F}^\top \mathbf{D}_{\tilde{\mathbf{p}}} (\mathbf{r} - g) \quad \in \mathbb{R}^{\dim(\mathbf{w})}. \end{aligned} \quad (9)$$

The minimizer \mathbf{w}^* in (7) involves \mathbf{X}^{-1} , which exists whenever Assumption 2.1 is satisfied, and the singularity of $(\mathbf{I} - \mathbf{P})$ is remedied. For example, by introducing an eligibility factor $\lambda \in (0, 1)$ such that \mathbf{X} then involves $(\mathbf{I} - \mathbf{P}^{(\lambda)})$, where $\mathbf{P}^{(\lambda)} := (1 - \lambda) \sum_{\tau=0}^{\infty} \lambda^\tau \mathbf{P}^{\tau+1}$. Another technique is replacing \mathbf{X} altogether with its non-singular approximation by some perturbation (Tsitsiklis and Roy, 1999, Lemma 7, Corollary 1). Note that $(\mathbf{I} - \mathbf{P})$ is not invertible (Puterman, 1994, p596).

An LSTD-based method approximately computes the minimizer \mathbf{w}^* in (7) by the sample means of \mathbf{X} and \mathbf{y} according to (8) and (9), respectively. That is,

$$\hat{\mathbf{w}}^* = \hat{\mathbf{X}}^{-1} \hat{\mathbf{y}} = \left(\frac{1}{n_{\text{sam}}} \sum_{i=1}^{n_{\text{sam}}} \mathbf{f}(s_i) (\mathbf{f}(s_i) - \mathbf{f}(s'_i))^\top \right)^{-1} \left(\frac{1}{n_{\text{sam}}} \sum_{i=1}^{n_{\text{sam}}} (r_i - g) \mathbf{f}(s_i) \right), \quad (10)$$

where n_{sam} denotes the number of state s_i , next state s'_i , and reward r_i samples, which are collected by the agent through interaction with its environment. Typically in practice, $\hat{\mathbf{X}} \leftarrow \hat{\mathbf{X}} + \epsilon \mathbf{I}$ for some small positive $\epsilon > 0$ in order to ensure the approximation matrix $\hat{\mathbf{X}}$ is invertible.

One interesting property of LSTD based on p^* is that its minimizer (7) is also the solution of the semi-gradient TD method for recurrent MDPs (Tsitsiklis and Roy, 1999). This method minimizes the weighted mean squared error (MSE) as follows,

$$\tilde{e}_{\text{MS}}(\mathbf{w}) := \sum_{s \in \mathcal{S}} \tilde{p}(s) [v(s) - \hat{v}(s; \mathbf{w})]^2 = \|\mathbf{v} - \hat{\mathbf{v}}(\mathbf{w})\|_{\tilde{\mathbf{p}}}^2 = [\mathbf{v} - \hat{\mathbf{v}}(\mathbf{w})]^\top \mathbf{D}_{\tilde{\mathbf{p}}} [\mathbf{v} - \hat{\mathbf{v}}(\mathbf{w})], \quad (11)$$

where \mathbf{v} denotes the true (ground-truth) value, while $\tilde{\mathbf{p}} \leftarrow \mathbf{p}^*$ and $\mathbf{D}_{\tilde{\mathbf{p}}}$ are the state distribution and the corresponding diagonal matrix, respectively. The semi-gradient TD method follows the stochastic gradient descent (SGD) for updating its parameter \mathbf{w} . For linear parameterization (2) such that $\nabla \hat{v}(s; \mathbf{w}) = \mathbf{f}(s)$, the SGD update rule for an approximation iterate $\hat{\mathbf{w}}^* \approx \mathbf{w}^*$ is given by

$$\underbrace{\hat{\mathbf{w}}^* \leftarrow \hat{\mathbf{w}}^* - \alpha \hat{\nabla} \tilde{e}_{\text{MS}}(\hat{\mathbf{w}}^*)}_{\text{cf. the LSTD estimator in (10)}}, \quad \text{with } \hat{\nabla} \tilde{e}_{\text{MS}}(\hat{\mathbf{w}}^*) := - \underbrace{\left(r(s) - g + \hat{v}(s'; \hat{\mathbf{w}}^*) - \hat{v}(s; \hat{\mathbf{w}}^*) \right)}_{\approx v(s) \text{ based on (3)}} \mathbf{f}(s), \quad (12)$$

where α is some positive learning rate and $\hat{\nabla} \tilde{e}_{\text{MS}}$ is the stochastic estimate of the gradient of \tilde{e}_{MS} (11) by one current state s and one next state s' sampled from p^* and $p(\cdot|s)$, respectively. Since the true $v(s)$ is unknown in RL, an approximation is substituted for it in (12) only after taking the gradient (hence, the term semi-gradient¹). Such approximation is based on the Bellman equation (3). It can be shown that the approximation iterate $\hat{\mathbf{w}}^*$ (12) converges to the LSTD's minimizer \mathbf{w}^* in (7), for which \mathbf{w}^* is called the TD fixed point (Sutton and Barto, 2018, p206). Note that a semi-gradient TD method needs the specification of the learning rate α and the initial value for $\hat{\mathbf{w}}^*$.

¹In contrast, LSTD methods are based on (true) gradients of the error function $\tilde{e}_{\mathbb{P}\mathbb{B}}$. This is possible since $\nabla \tilde{e}_{\mathbb{P}\mathbb{B}}$ does not involve the true value $v(s)$, see (18).

3 Seminorm LSTD approximators

In this section, we present an LSTD approximator that minimizes $\tilde{e}_{\mathbb{P}\mathbb{B}}$ (4), whose state distribution \tilde{p} does not necessarily have the whole state set as its support, i.e. $\tilde{p}(s) \geq 0, \forall s \in \mathcal{S}$. This \tilde{p} induces a positive semidefinite (PSD) diagonal matrix $D_{\tilde{p}}$, hence a seminorm $\tilde{e}_{\mathbb{P}\mathbb{B}}$. Consequently, minimizing $\tilde{e}_{\mathbb{P}\mathbb{B}}$ and deriving its projector $\tilde{\mathbb{P}}$ (5) require solving $D_{\tilde{p}}$ -seminorm LS problems. We call the corresponding state-value approximator based on such $\tilde{e}_{\mathbb{P}\mathbb{B}}$ as a *seminorm LSTD*.

A seminorm LSTD is useful for unichain MCs with multiple transient and recurrent states (and with certain reward structures). For example, since each state type has different timing (transient states are visited at the outset before absorption, whereas recurrent states in the long-run), a proper \tilde{p} is different for each type so that the support of a proper type-specific \tilde{p} only contains a subset of the state set; inducing a seminorm $\tilde{e}_{\mathbb{P}\mathbb{B}}$. It is proper in that it provides reasonable weighting for the state-wise error terms in (4) and (5), and that it enables state sampling in (8) and (9). More importantly, a seminorm LSTD facilitates the derivation of a general approximation procedure (see Sec 4).

The main result of this Section is a sampling-enabler expression for the minimizer of $\tilde{e}_{\mathbb{P}\mathbb{B}}$ of a seminorm LSTD. It is presented in Thm 3.1 (Sec 3.2). For that, the preceding Sec 3.1 contains the projection operator for the seminorm $\tilde{e}_{\mathbb{P}\mathbb{B}}$ and two necessary lemmas for the minimizer.

3.1 Necessary components for the error function and the minimizer

We begin with the projection operator $\tilde{\mathbb{P}}$ that involves the $D_{\tilde{p}}$ -seminorm. It is stated in Lemma 3.1 below. Recall that $\tilde{\mathbb{P}}$ projects any value v onto the space of representable parameterized approximators. To proceed, we need the following Def 3.1.

Definition 3.1. *Given a matrix $A \in \mathbb{R}^{m \times n}$, then its Moore-Penrose pseudoinverse $A^\dagger \in \mathbb{R}^{n \times m}$ is the unique matrix such that (i) $AA^\dagger A = A$, (ii) $A^\dagger AA^\dagger = A^\dagger$, (iii) $(AA^\dagger)^\top = AA^\dagger$, and (iv) $(A^\dagger A)^\top = A^\dagger A$. See [Campbell and Meyer \(2009, Def 1.1.3\)](#).*

Lemma 3.1. *The projection operator $\tilde{\mathbb{P}}$ involving the $D_{\tilde{p}}$ -seminorm is given by*

$$\tilde{\mathbb{P}} = \mathbf{F} \mathbf{Z}^\dagger \mathbf{F}^\top D_{\tilde{p}}, \quad \text{where } \mathbf{Z} := \mathbf{F}^\top D_{\tilde{p}} \mathbf{F} = \mathbb{E}_{S \sim \tilde{p}}[\mathbf{f}(S) \mathbf{f}(S)^\top] \in \mathbb{R}^{\dim(w) \times \dim(w)}.$$

Here, the state distribution \tilde{p} may have zero probabilities for some states, i.e. $\tilde{p}(s) \geq 0, \forall s \in \mathcal{S}$. The superscript \dagger indicates the Moore-Penrose pseudoinverse (Def 3.1).

Proof. The projection operator $\tilde{\mathbb{P}}$ is a matrix that satisfies $\tilde{\mathbb{P}}v = \mathbf{F}w^\diamond$, where

$$w^\diamond = \underset{w \in \mathcal{W}}{\operatorname{argmin}} \left\{ \|\{\hat{v} = \mathbf{F}w\} - v\|_{D_{\tilde{p}}}^2 = \sum_{s \in \mathcal{S}} [\tilde{p}^{\frac{1}{2}}(s)]^2 [\hat{v}(s; w) - v(s)]^2 = \|D_{\tilde{p}}^{\frac{1}{2}}(\mathbf{F}w - v)\|_2^2 \right\}.$$

Finding w^\diamond amounts to solving for

$$\begin{aligned} & \text{the } D_{\tilde{p}}\text{-seminorm LS solutions of } \mathbf{F}w = v, \text{ or equivalently,} \\ & \text{the Euclidean-norm LS solutions of } D_{\tilde{p}}^{\frac{1}{2}} \mathbf{F}w = D_{\tilde{p}}^{\frac{1}{2}} v. \end{aligned} \quad (13)$$

The latter has the following general form ([Ben-Israel and Greville, 2003, p106](#)),

$$\begin{aligned} w^\diamond &= [D_{\tilde{p}}^{\frac{1}{2}} \mathbf{F}]^\dagger D_{\tilde{p}}^{\frac{1}{2}} v + [I - (D_{\tilde{p}}^{\frac{1}{2}} \mathbf{F})^\dagger (D_{\tilde{p}}^{\frac{1}{2}} \mathbf{F})] c \\ &= \underbrace{[(D_{\tilde{p}}^{\frac{1}{2}} \mathbf{F})^\top D_{\tilde{p}}^{\frac{1}{2}} \mathbf{F}]^\dagger (D_{\tilde{p}}^{\frac{1}{2}} \mathbf{F})^\top D_{\tilde{p}}^{\frac{1}{2}} v}_{[\mathbf{F}^\top D_{\tilde{p}} \mathbf{F}]^\dagger \mathbf{F}^\top D_{\tilde{p}} v} + [I - ((D_{\tilde{p}}^{\frac{1}{2}} \mathbf{F})^\top D_{\tilde{p}}^{\frac{1}{2}} \mathbf{F})^\dagger ((D_{\tilde{p}}^{\frac{1}{2}} \mathbf{F})^\top D_{\tilde{p}}^{\frac{1}{2}} \mathbf{F})] c, \end{aligned} \quad (14)$$

for an arbitrary vector $c \in \mathbb{R}^{\dim(w)}$. Since the gradient at w^\diamond vanishes (a necessary condition for the minimizer), it can be shown that w^\diamond is also the solution of the normal equation of (13) as in ([Campbell and Meyer, 2009, Thm 2.1.2](#)). That is,

$$\begin{aligned} \nabla \|\mathbf{F}w - v\|_{D_{\tilde{p}}}^2 &= 2\mathbf{F}^\top D_{\tilde{p}}(\mathbf{F}w^\diamond - v) = 0 && \text{(Whenever } w = w^\diamond) \\ &\iff \mathbf{F}^\top D_{\tilde{p}} \mathbf{F}w^\diamond = \mathbf{F}^\top D_{\tilde{p}} v && \text{(cf. (14))} \\ &\iff (D_{\tilde{p}}^{\frac{1}{2}} \mathbf{F})^\top D_{\tilde{p}}^{\frac{1}{2}} \mathbf{F}w^\diamond = (D_{\tilde{p}}^{\frac{1}{2}} \mathbf{F})^\top D_{\tilde{p}}^{\frac{1}{2}} v. && \text{(The normal equation of (13))} \end{aligned}$$

By setting \mathbf{c} to zero in (14), we obtain one $D_{\tilde{\mathcal{P}}}$ -seminorm LS solution, denoted as $\tilde{\mathbf{w}}^\diamond$. The projection then takes the form of

$$\tilde{\mathbb{P}}\mathbf{v} = \mathbf{F}\tilde{\mathbf{w}}^\diamond = \mathbf{F}\{[\mathbf{F}^\top D_{\tilde{\mathcal{P}}}\mathbf{F}]^\dagger \mathbf{F}^\top D_{\tilde{\mathcal{P}}}\mathbf{v}\} = \mathbf{F}\{\mathbf{Z}^\dagger \mathbf{F}^\top D_{\tilde{\mathcal{P}}}\mathbf{v}\}, \quad \text{hence, } \tilde{\mathbb{P}} = \mathbf{F}\mathbf{Z}^\dagger \mathbf{F}^\top D_{\tilde{\mathcal{P}}}.$$

Note that this $\tilde{\mathbf{w}}^\diamond$ is not the minimal $D_{\tilde{\mathcal{P}}}$ -seminorm $D_{\tilde{\mathcal{P}}}$ -LS solution, i.e. $\tilde{\mathbf{w}}^\diamond \neq \operatorname{argmin}_{\mathbf{w}^\diamond} \|\mathbf{w}^\diamond\|_{D_{\tilde{\mathcal{P}}}}$, see Proszynski and Sosnowski (1995, Thm 2). This concludes the proof. \blacksquare

The next Lemma 3.2 describes the relevant properties of matrix \mathbf{Z} , which emerges during the foregoing derivation of $\tilde{\mathbb{P}}$. This is essential because \mathbf{Z} and its pseudoinverse \mathbf{Z}^\dagger (along with its matrix square root) play an important role in the derivation of the minimizer of $\tilde{e}_{\mathbb{P}\mathbb{B}}$ (see Thm 3.1).

Lemma 3.2. *These real matrices \mathbf{Z} , \mathbf{Z}^\dagger , and $\mathbf{Z}^{\dagger/2}$ are symmetric positive semidefinite (PSD). Here, $\mathbf{Z} := \mathbf{F}^\top D_{\tilde{\mathcal{P}}}\mathbf{F}$, and $\mathbf{Z}^{\dagger/2} := (\mathbf{Z}^\dagger)^{\frac{1}{2}} = \sqrt{\mathbf{Z}^\dagger}$, which is the matrix square root of \mathbf{Z}^\dagger .*

Proof. First, \mathbf{Z} involves a PSD diagonal matrix $D_{\tilde{\mathcal{P}}} = (D_{\tilde{\mathcal{P}}}^{\frac{1}{2}})^2$ with its unique matrix square root $D_{\tilde{\mathcal{P}}}^{\frac{1}{2}}$. Let $\mathbf{G} := D_{\tilde{\mathcal{P}}}^{\frac{1}{2}}\mathbf{F}$. Expressing \mathbf{Z} as a Gram matrix gives $\mathbf{Z}^\top = (\mathbf{G}^\top \mathbf{G})^\top = \mathbf{G}^\top \mathbf{G} = \mathbf{Z}$, which shows that \mathbf{Z} is symmetric. Moreover,

$$\mathbf{u}^\top \mathbf{Z} \mathbf{u} = \mathbf{u}^\top \mathbf{F}^\top D_{\tilde{\mathcal{P}}}^{\frac{1}{2}} D_{\tilde{\mathcal{P}}}^{\frac{1}{2}} \mathbf{F} \mathbf{u} = (D_{\tilde{\mathcal{P}}}^{\frac{1}{2}} \mathbf{F} \mathbf{u})^\top (D_{\tilde{\mathcal{P}}}^{\frac{1}{2}} \mathbf{F} \mathbf{u}) = \|D_{\tilde{\mathcal{P}}}^{\frac{1}{2}} \mathbf{F} \mathbf{u}\|_2^2 \geq 0, \quad \forall \mathbf{u} \in \mathbb{R}^{\dim(\mathbf{f})}. \quad (15)$$

Hence, \mathbf{Z} is symmetric positive semidefinite (PSD).

Second, let the singular value decomposition (SVD) of \mathbf{Z} is given by $\mathbf{M}D_{\tilde{\sigma}}\mathbf{N}^\top$. Then, we have

$$\begin{aligned} \mathbf{Z}\mathbf{Z}^\top &= \mathbf{M}D_{\tilde{\sigma}}\mathbf{N}^\top \mathbf{N}D_{\tilde{\sigma}}\mathbf{M}^\top = \mathbf{M}D_{\tilde{\sigma}}^2\mathbf{M}^\top, & (\text{Since } \mathbf{N} \text{ is orthogonal}) \\ \mathbf{Z}^\top \mathbf{Z} &= \mathbf{N}D_{\tilde{\sigma}}\mathbf{M}^\top \mathbf{M}D_{\tilde{\sigma}}\mathbf{N}^\top = \mathbf{N}D_{\tilde{\sigma}}^2\mathbf{N}^\top. & (\text{Since } \mathbf{M} \text{ is orthogonal}) \end{aligned}$$

Because \mathbf{Z} is symmetric (hence, normal), we have $\mathbf{Z}\mathbf{Z}^\top = \mathbf{Z}^\top \mathbf{Z} = \mathbf{Z}^2$. Thus, $\mathbf{M} = \mathbf{N}$ whose columns are the orthogonal eigenvectors of \mathbf{Z}^2 , which are then normalized to become unit vectors in order to have an orthogonal matrix \mathbf{M} . By SVD, the singular value diagonal matrix $D_{\tilde{\sigma}}$ contains the squared roots of eigenvalues of \mathbf{Z}^2 .

Let μ be the eigenvalue of \mathbf{Z} with eigenvector \mathbf{u} , then

$$\mathbf{Z}\mathbf{u} = \mu\mathbf{u}, \quad \text{and} \quad \mathbf{Z}^2\mathbf{u} = \mathbf{Z}(\mathbf{Z}\mathbf{u}) = \mathbf{Z}(\mu\mathbf{u}) = \mu(\mathbf{Z}\mathbf{u}) = \mu(\mu\mathbf{u}) = \mu^2\mathbf{u},$$

which shows that \mathbf{u} is an eigenvector of \mathbf{Z}^2 with the eigenvalue μ^2 . This holds for all eigenvalues of \mathbf{Z} , which become the diagonal entries of $D_{\tilde{\sigma}}$ (such eigenvalues are non-negative since \mathbf{Z} is PSD). Moreover, because \mathbf{Z} is symmetric, both \mathbf{Z} and \mathbf{Z}^2 have the same set of orthogonal eigenvectors, which becomes the columns of \mathbf{M} . Thus, the eigen (spectral) decomposition (EigD) of \mathbf{Z} , namely $\mathbf{U}D_{\tilde{\mu}}\mathbf{U}^\top$, is also a valid SVD. Consequently,

$$\mathbf{Z}^\dagger = \underbrace{(\mathbf{M}D_{\tilde{\sigma}}\mathbf{N}^\top)^\dagger}_{\text{SVD of } \mathbf{Z}} = \underbrace{(\mathbf{U}D_{\tilde{\mu}}\mathbf{U}^\top)^\dagger}_{\text{EigD of } \mathbf{Z}} = \mathbf{U}D_{\tilde{\mu}}^\dagger\mathbf{U}^\top = \mathbf{U}D_{\tilde{\mu}}^{\dagger/2}D_{\tilde{\mu}}^{\dagger/2}\mathbf{U}^\top = (D_{\tilde{\mu}}^{\dagger/2}\mathbf{U}^\top)^\top(D_{\tilde{\mu}}^{\dagger/2}\mathbf{U}^\top), \quad (16)$$

where $D_{\tilde{\mu}}^\dagger$ is obtained by taking the reciprocal of non-zeroes entries of $D_{\tilde{\mu}}$. Thus, \mathbf{Z}^\dagger can be expressed as a Gram matrix, which is always PSD as shown before in (15). Since \mathbf{Z}^\dagger is PSD, there exists exactly one (symmetric) PSD matrix $\mathbf{Z}^{\dagger/2}$ such that $\mathbf{Z}^\dagger = \mathbf{Z}^{\dagger/2}\mathbf{Z}^{\dagger/2}$. From (16) above, we have $\mathbf{Z}^{\dagger/2} = D_{\tilde{\mu}}^{\dagger/2}\mathbf{U}^\top$. This concludes the proof, whose alternatives can be found in (Lewis and Newman, 1968, Corollary 3; Harville, 1997, Thm 20.5.3). \blacksquare

3.2 The sampling-enabler expression for the minimizer

The core component of a seminorm LSTD is the minimizer $\tilde{\mathbf{w}}^*$ of its error $\tilde{e}_{\mathbb{P}\mathbb{B}}$, which involves a PSD matrix $D_{\tilde{\mathcal{P}}}$. In particular for model-free RL, we need an expression of $\tilde{\mathbf{w}}^*$ that enables sampling based approximation, akin to (7). By utilizing Lemmas 3.1 and 3.2 from the previous Sec 3.1, we are now ready to derive such a sampling-enabler expression. It is stated in the following Thm 3.1.

Theorem 3.1. *One minimizer of the error $\tilde{e}_{\mathbb{P}\mathbb{B}}(\mathbf{w})$ in (4), which involves a state distribution \tilde{p} with $\tilde{p}(s) \geq 0, \forall s \in \mathcal{S}$ (hence, $\tilde{e}_{\mathbb{P}\mathbb{B}}$ is a seminorm with a PSD diagonal matrix $\mathbf{D}_{\tilde{p}}$), is given by*

$$\tilde{\mathbf{w}}^* = (\mathbf{X}^\top \mathbf{Z}^\dagger \mathbf{X})^\dagger \mathbf{X}^\top \mathbf{Z}^\dagger \mathbf{y} = (\mathbf{Z}^{\dagger/2} \mathbf{X})^\dagger \mathbf{Z}^{\dagger/2} \mathbf{y}, \quad \text{where} \quad (17)$$

$$\begin{aligned} \mathbf{X} &:= \mathbb{E}_{S \sim \tilde{p}, S' \sim p(\cdot|s)} [\mathbf{f}(S)(\mathbf{f}(S) - \mathbf{f}(S'))^\top], \quad (\text{with state feature } \mathbf{f}(s) \text{ and one-step transition } p) \\ \mathbf{Z} &:= \mathbb{E}_{S \sim \tilde{p}} [\mathbf{f}(S)\mathbf{f}(S)^\top], \quad \text{and} \quad (\text{with state feature } \mathbf{f}(s) \text{ as above}) \\ \mathbf{y} &:= \mathbb{E}_{S \sim \tilde{p}} [(r(S) - g)\mathbf{f}(S)]. \quad (\text{with state reward } r(s), \text{ gain } g \text{ and } \mathbf{f}(s) \text{ as above}) \end{aligned}$$

Here, $p(\cdot|s)$ denotes the next state conditional distribution (i.e. the one-step state transition distribution given the current state s). Note that we abuse the notations \mathbf{X} and \mathbf{y} , which are also used in (8) and (9) but with a different state distribution.

Pertaining to Thm 3.1, we remark that the formula simplification in (17) is crucial because the resulting expression enables unbiased sampling-based estimation for the minimizer $\tilde{\mathbf{w}}^*$ in model-free RL. This is possible because the last expression in (17) involves only one factor of \mathbf{X} . In contrast, the expression before simplification has three factors of \mathbf{X} , hence it does not enable such unbiased estimation for $\tilde{\mathbf{w}}^*$. The reason stems from the fact that \mathbf{X} depends on the next-state random variable through $\mathbb{E}_{p(\cdot|s)}[\mathbf{f}(S')]$, which leads to a similar situation as described by Sutton and Barto (2018, p272). They explain that multiple independent samples of next states are required to obtain an unbiased estimate of the product of multiple factors that involve expectations of next states. Such independent next-state samples are only available in deterministic transition (where the next state is not random), or in simulation where the agent can roll-back from any state to its previous state. This sampling requirement cannot be accommodated in model-free RL settings since the agent cannot roll-back to its previous state and transitions are generally stochastic.

In addition, we also remark that the simplification in (17) is carried out without introducing any error (putting aside errors due to numerical computation). In comparison, simplifying $\tilde{\mathbf{w}}^*$ (to involve only one factor of \mathbf{X}) through the reverse order law for the pseudoinverse is possible but with some errors because the identity $(\mathbf{X}^\top \mathbf{Z}^\dagger \mathbf{X})^\dagger = \mathbf{X}^\dagger \mathbf{Z} \mathbf{X}^{\top\dagger}$ requires strict conditions (Hartwig, 1986; Tian, 2019). Two example simplifications with errors are as follows,

- by orthogonal approximation $\mathbf{X}_\perp \approx \mathbf{X}$ (where $\mathbf{X}_\perp^\dagger = \mathbf{X}_\perp^{-1} = \mathbf{X}_\perp^\top$) and the identity $(\mathbf{X}_\perp^\top \mathbf{Z}^\dagger \mathbf{X}_\perp)^\dagger = \mathbf{X}_\perp^\top \mathbf{Z} \mathbf{X}_\perp$ (Campbell and Meyer, 2009, Theorem 1.2.1: 7) such that

$$\tilde{\mathbf{w}}^* = (\mathbf{X}^\top \mathbf{Z}^\dagger \mathbf{X})^\dagger \mathbf{X}^\top \mathbf{Z}^\dagger \mathbf{y} \approx (\mathbf{X}_\perp^\top \mathbf{Z}^\dagger \mathbf{X}_\perp)^\dagger \mathbf{X}_\perp^\top \mathbf{Z}^\dagger \mathbf{y} = \mathbf{X}_\perp^\top \mathbf{Z} \mathbf{Z}^\dagger \mathbf{y},$$

- by nullifying the constant matrices \mathbf{C}_1 and \mathbf{C}_2 (in below expression) such that

$$\begin{aligned} \tilde{\mathbf{w}}^* &= (\mathbf{X}^\top \mathbf{Z}^\dagger \mathbf{X})^\dagger \mathbf{X}^\top \mathbf{Z}^\dagger \mathbf{y} = (\mathbf{X}^\dagger \mathbf{Z} \mathbf{X}^{\top\dagger} + \mathbf{C}_1) \mathbf{X}^\top \mathbf{Z}^\dagger \mathbf{y} \\ &\approx \mathbf{X}^\dagger \mathbf{Z} \mathbf{X}^{\top\dagger} \mathbf{X}^\top \mathbf{Z}^\dagger \mathbf{y} = \mathbf{X}^\dagger \mathbf{Z} (\mathbf{I} + \mathbf{C}_2) \mathbf{Z}^\dagger \mathbf{y} \approx \mathbf{X}^\dagger \mathbf{Z} \mathbf{Z}^\dagger \mathbf{y}. \end{aligned}$$

Finally, we present the proof for Thm 3.1 about the minimizer $\tilde{\mathbf{w}}^*$ below.

Proof. (of Thm 3.1) The MSBPE error $\tilde{e}_{\mathbb{P}\mathbb{B}}$ in (4) can be expressed as follows,

$$\begin{aligned} \tilde{e}_{\mathbb{P}\mathbb{B}}(\mathbf{w}) &= \|\hat{\mathbf{v}} - \tilde{\mathbb{P}}\mathbb{B}\hat{\mathbf{v}}\|_{\mathbf{D}_{\tilde{p}}}^2 = \|\tilde{\mathbb{P}}\hat{\mathbf{v}} - \tilde{\mathbb{P}}\mathbb{B}\hat{\mathbf{v}}\|_{\mathbf{D}_{\tilde{p}}}^2 = \|\tilde{\mathbb{P}}[\hat{\mathbf{v}} - \mathbb{B}\hat{\mathbf{v}}]\|_{\mathbf{D}_{\tilde{p}}}^2 \quad (\text{Recall } \hat{\mathbf{v}} \text{ is representable}) \\ &= \{\tilde{\mathbb{P}}[\hat{\mathbf{v}} - \mathbb{B}\hat{\mathbf{v}}]\}^\top \mathbf{D}_{\tilde{p}} \{\tilde{\mathbb{P}}[\hat{\mathbf{v}} - \mathbb{B}\hat{\mathbf{v}}]\} = [\hat{\mathbf{v}} - \mathbb{B}\hat{\mathbf{v}}]^\top \{\tilde{\mathbb{P}}^\top \mathbf{D}_{\tilde{p}} \tilde{\mathbb{P}}\} [\hat{\mathbf{v}} - \mathbb{B}\hat{\mathbf{v}}] \\ &= [\hat{\mathbf{v}} - \mathbb{B}\hat{\mathbf{v}}]^\top \{\mathbf{F} \mathbf{Z}^\dagger \mathbf{F}^\top \mathbf{D}_{\tilde{p}}\}^\top \mathbf{D}_{\tilde{p}} \{\mathbf{F} \mathbf{Z}^\dagger \mathbf{F}^\top \mathbf{D}_{\tilde{p}}\} [\hat{\mathbf{v}} - \mathbb{B}\hat{\mathbf{v}}] \quad (\text{Expand } \tilde{\mathbb{P}} \text{ from Lemma 3.1}) \\ &= [\hat{\mathbf{v}} - \mathbb{B}\hat{\mathbf{v}}]^\top \{\mathbf{D}_{\tilde{p}} \mathbf{F} \mathbf{Z}^\dagger \mathbf{F}^\top\} \mathbf{D}_{\tilde{p}} \{\mathbf{F} \mathbf{Z}^\dagger \mathbf{F}^\top \mathbf{D}_{\tilde{p}}\} [\hat{\mathbf{v}} - \mathbb{B}\hat{\mathbf{v}}] \quad (\mathbf{Z}^\dagger \text{ is symmetric (Lemma 3.2)}) \\ &= \{\mathbf{F}^\top \mathbf{D}_{\tilde{p}} [\hat{\mathbf{v}} - \mathbb{B}\hat{\mathbf{v}}]\}^\top \mathbf{Z}^\dagger \{\mathbf{F}^\top \mathbf{D}_{\tilde{p}} \mathbf{F}\} \mathbf{Z}^\dagger \{\mathbf{F}^\top \mathbf{D}_{\tilde{p}} [\hat{\mathbf{v}} - \mathbb{B}\hat{\mathbf{v}}]\} \\ &= \{\mathbf{F}^\top \mathbf{D}_{\tilde{p}} [\hat{\mathbf{v}} - \mathbb{B}\hat{\mathbf{v}}]\}^\top \mathbf{Z}^\dagger \{\mathbf{F}^\top \mathbf{D}_{\tilde{p}} [\hat{\mathbf{v}} - \mathbb{B}\hat{\mathbf{v}}]\} \quad (\text{Apply the condition (ii) in Def 3.1}) \\ &= \|\mathbf{F}^\top \mathbf{D}_{\tilde{p}} [\hat{\mathbf{v}} - \mathbb{B}\hat{\mathbf{v}}]\|_{\mathbf{Z}^\dagger}^2 \quad (\mathbf{Z}^\dagger \text{ is PSD (Lemma 3.2), hence } \mathbf{Z}^\dagger\text{-seminorm}) \\ &= \|\mathbf{F}^\top \mathbf{D}_{\tilde{p}} [\mathbf{F}\mathbf{w} - \mathbf{P}\mathbf{F}\mathbf{w} - (\mathbf{r} - g)]\|_{\mathbf{Z}^\dagger}^2 \quad (\text{Expand } \hat{\mathbf{v}} \text{ from (2) and } \mathbb{B} \text{ from (3)}) \\ &= \|\mathbf{F}^\top \mathbf{D}_{\tilde{p}} \mathbf{F}\mathbf{w} - \mathbf{F}^\top \mathbf{D}_{\tilde{p}} \mathbf{P}\mathbf{F}\mathbf{w} - \mathbf{F}^\top \mathbf{D}_{\tilde{p}} (\mathbf{r} - g)\|_{\mathbf{Z}^\dagger}^2 \\ &= \|\underbrace{\mathbf{F}^\top \mathbf{D}_{\tilde{p}} (\mathbf{I} - \mathbf{P}) \mathbf{F}}_{\mathbf{X}} \mathbf{w} - \underbrace{\mathbf{F}^\top \mathbf{D}_{\tilde{p}} (\mathbf{r} - g)}_{\mathbf{y}}\|_{\mathbf{Z}^\dagger}^2 = \|\mathbf{X}\mathbf{w} - \mathbf{y}\|_{\mathbf{Z}^\dagger}^2. \end{aligned}$$

The above steps are inspired by [Dann et al. \(2014, Appendix A\)](#) who derived the (norm) LSTD based on the stationary state distribution p^* for the discounted-reward value function for recurrent MDPs.

Therefore, minimizing $\tilde{e}_{\mathbb{P}\mathbb{B}}$ (which is a seminorm as $D_{\tilde{p}}$ is PSD) amounts to solving for

$$\begin{aligned} & \text{the } \mathbf{Z}^\dagger\text{-seminorm LS solutions of } \mathbf{X}\mathbf{w} = \mathbf{y}, \quad \text{or equivalently,} \\ & \text{the Euclidean-norm LS solutions of } \mathbf{Z}^{\dagger/2}\mathbf{X}\mathbf{w} = \mathbf{Z}^{\dagger/2}\mathbf{y}. \end{aligned} \quad (\text{Similar to (13)})$$

Taking the gradient of $\tilde{e}_{\mathbb{P}\mathbb{B}}$ and setting it to zero for a minimizer $\tilde{\mathbf{w}}^*$ gives

$$\nabla \tilde{e}_{\mathbb{P}\mathbb{B}}(\mathbf{w}) = \nabla \|\mathbf{X}\mathbf{w} - \mathbf{y}\|_{\mathbf{Z}^\dagger}^2 = 2\mathbf{X}^\top \mathbf{Z}^\dagger (\mathbf{X}\mathbf{w} - \mathbf{y}) \stackrel{\text{set}}{=} \mathbf{0} \iff \mathbf{X}^\top \mathbf{Z}^\dagger \mathbf{X} \tilde{\mathbf{w}}^* = \mathbf{X}^\top \mathbf{Z}^\dagger \mathbf{y}. \quad (18)$$

In a similar fashion as the derivation of $\tilde{\mathbb{P}}$ (Lemma 3.1), one solution for (18) is given by

$$\begin{aligned} \tilde{\mathbf{w}}^* &= (\mathbf{X}^\top \mathbf{Z}^\dagger \mathbf{X})^\dagger \mathbf{X}^\top \mathbf{Z}^\dagger \mathbf{y} = (\mathbf{X}^\top \mathbf{Z}^{\dagger/2} \mathbf{Z}^{\dagger/2} \mathbf{X})^\dagger \mathbf{X}^\top \mathbf{Z}^{\dagger/2} \mathbf{Z}^{\dagger/2} \mathbf{y} && (\text{See (16)}) \\ &= (\mathbf{L}^\top \mathbf{L})^\dagger \mathbf{L}^\top \mathbf{Z}^{\dagger/2} \mathbf{y} \quad (\text{Let } \mathbf{L} := \mathbf{Z}^{\dagger/2} \mathbf{X}, \text{ so } \mathbf{L}^\top = \mathbf{X}^\top \mathbf{Z}^{\dagger/2} \text{ as } \mathbf{Z}^{\dagger/2} \text{ is symmetric (Lemma 3.2)}) \\ &= \mathbf{L}^\dagger \mathbf{Z}^{\dagger/2} \mathbf{y} && (\text{Since } (\mathbf{L}^\top \mathbf{L})^\dagger \mathbf{L}^\top = \mathbf{L}^\dagger \text{ (Campbell and Meyer, 2009, Thm 1.2.1: 6)}) \\ &= (\mathbf{Z}^{\dagger/2} \mathbf{X})^\dagger \mathbf{Z}^{\dagger/2} \mathbf{y}, && (\text{Expand } \mathbf{L}) \end{aligned}$$

which can be plugged-in back to the LHS of (18) to confirm that

$$\mathbf{X}^\top \mathbf{Z}^\dagger \mathbf{X} (\tilde{\mathbf{w}}^*) = \mathbf{X}^\top \mathbf{Z}^{\dagger/2} \mathbf{Z}^{\dagger/2} \mathbf{X} (\mathbf{L}^\dagger \mathbf{Z}^{\dagger/2} \mathbf{y}) = \{\mathbf{L}^\top \mathbf{L} \mathbf{L}^\dagger\} \mathbf{Z}^{\dagger/2} \mathbf{y} = \{\mathbf{L}^\top\} \mathbf{Z}^{\dagger/2} \mathbf{y} = \mathbf{X}^\top \mathbf{Z}^{\dagger/2} \mathbf{Z}^{\dagger/2} \mathbf{y}.$$

Here, we rely on the identity of $\mathbf{L}^\top \mathbf{L} \mathbf{L}^\dagger = \mathbf{L}^\top$ ([Campbell and Meyer, 2009, Thm 1.2.1: 4](#)). This concludes the proof. \blacksquare

4 A general procedure for LSTD-based policy evaluation

Equipped with seminorm LSTD (Sec 3), we are now ready to devise a general unifying procedure for LSTD-based policy evaluation, which leads to a system of LSTD approximators, as illustrated in Fig 1. The proposed procedure is formally presented in Def 4.4, for which we need the definitions of its main components as follows.

Definition 4.1. A *timestep neighborhood*, denoted as \mathcal{N} , is an ordered set of consecutive timesteps from an anchor timestep t to $(t + |\mathcal{N}| - 1)$. Every neighborhood \mathcal{N} has a unique anchor t (i.e. the earliest timestep in \mathcal{N}). Hence, the notation \mathcal{N}_t denotes a neighborhood anchored at t . The non-anchor member of \mathcal{N}_t , if any, is called a neighbor. Hence, every anchor has $(|\mathcal{N}_t| - 1)$ neighbors.

Definition 4.2. A *state probability distribution of a neighborhood \mathcal{N}_t* , denoted as \bar{p}_t , is a lumpsum of stepwise state probabilities p^τ from $\tau = t$ to $(t + |\mathcal{N}| - 1)$. That is,

$$\bar{p}_t(s) := \frac{1}{|\mathcal{N}_t|} \sum_{\tau=t}^{t+|\mathcal{N}_t|-1} p^\tau(s), \quad \text{with } p^\tau(s) = \mathbb{E}_{S_0 \sim \bar{p}}[p^\tau(s|s_0)], \quad \forall s \in \mathcal{S}, \quad (19)$$

where $p^\tau(s|s_0) := \Pr\{S_\tau = s | S_0 = s_0\}$, which indicates the probability of visiting the state s in τ timesteps from an initial state s_0 . This $p^\tau(s|s_0)$ is equivalent to the $[s_0, s]$ -entry of \mathbf{P}^τ , which is the one-step transition matrix \mathbf{P} raised to the power of τ . That is, $p^\tau(s|s_0) = \mathbf{e}_{s_0}^\top \mathbf{P}^\tau \mathbf{e}_s$, where $\mathbf{e}_i \in \mathbb{R}^{|\mathcal{S}|}$ denotes the i -th standard basis vector. The s_0 -th row of \mathbf{P}^τ therefore contains the probability values of the stepwise conditional state distribution $p^\tau(\cdot|s_0)$.

Definition 4.3. The *support of a neighborhood \mathcal{N}_t* is defined as the support of its state distribution \bar{p}_t , denoted as $\mathcal{S}(\bar{p}_t)$. That is, $\mathcal{S}(\bar{p}_t) := \{s : \bar{p}_t(s) > 0, \forall s \in \mathcal{S}\} = \bigcup_{\tau=t}^{t+|\mathcal{N}_t|-1} \mathcal{S}(p^\tau) \subseteq \mathcal{S}$, where $\mathcal{S}(p^\tau)$ is the support of a stepwise state distribution p^τ . Note that $\mathcal{S}(\bar{p}_t)$ may be a proper subset of \mathcal{S} .

Definition 4.4. A general procedure for LSTD-based policy evaluation has three steps as follows.

1. Specify a number of timestep neighborhoods (Def 4.1) over the whole time-horizon.
2. Train a seminorm LSTD approximator (Sec 3.2) for every neighborhood \mathcal{N}_t . This approximator minimizes $\tilde{e}_{\mathbb{P}\mathbb{B}}$ that is based on the neighborhood state distribution $\tilde{p} \leftarrow \bar{p}_t$ (Def 4.2) and a desired type of policy value functions. It is termed as a seminorm LSTD- \tilde{p}_t .
3. Predict the state values at timestep τ using the approximator of a neighborhood \mathcal{N}_t where τ belongs (either as an anchor or a neighbor member of \mathcal{N}_t).

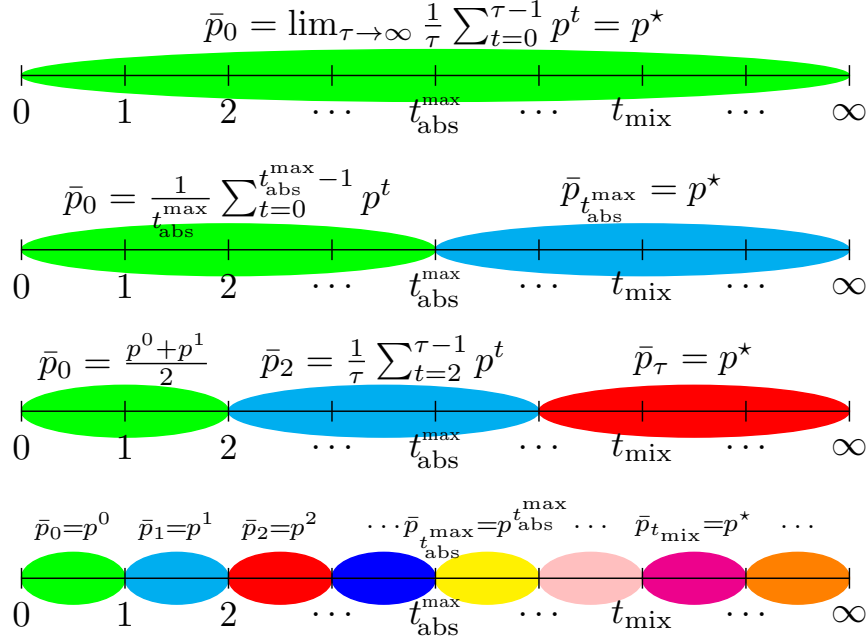


Figure 1: Illustrations of four systems (rows) of LSTD- \bar{p}_t approximators along the timestep line in infinite-horizon MDPs. The first system (top row) consists of only one approximator for one neighborhood anchored at $t = 0$, hence it is based on the stationary state distribution $\bar{p}_0 = p^*$. The second system consists of two approximators whose neighborhoods are anchored at $t = 0$ and $t = t_{\text{abs}}^{\text{max}}$, hence they are based on \bar{p}_0 and $\bar{p}_{t_{\text{abs}}^{\text{max}}} = p^*$. The third system consists of three approximators whose neighborhoods are anchored at $t = 0$, $t = 2$ and $t = \tau$ for some timestep τ . The fourth system consists of an infinity number of approximators (i.e. stepwise approximators), each is based on the stepwise state distribution $\bar{p}_t = p^t$.

The number of timestep neighborhoods (equivalently, the number of anchors or approximators) is denoted as n_a . This procedure forms a system of n_a seminorm LSTD- \bar{p}_t (as linear approximators).

This general procedure unifies two existing approaches to approximate policy evaluation (Sec 4.1), as summarized in Table 1. It also gives a spectrum of benefits by controlling the number of neighborhoods (Sec 4.2). More importantly, it enables value approximation for both transient and recurrent states in unichain MDPs, which is the main motivation for this work and is presented in Sec 5.

4.1 Existing approaches are special cases with one or two neighborhoods

In this section, we show that at least two existing LSTD-based approximators emerge as special cases of the general procedure (Def 4.4). These two are of interest because they have the essential components common to other LSTD-based approximators (see Table 1).

First is the average-reward LSTD (Yu and Bertsekas, 2009, Sec II.A), which was designed for recurrent MCs with rewards. This is a special case of the general procedure (Def 4.4) when $n_a \leftarrow 1$, yielding a single neighborhood anchored at the initial timestep $t = 0$ and with an infinite number of neighbors (due to an infinite time-horizon), as illustrated in Fig 1: top-row. The lumpsum state distribution of \mathcal{N}_0 is obtained by taking the limit of p^τ as τ approaches infinity in (19). This limiting distribution is by definition (6), equal to the stationary state distribution, that is $\bar{p}_0 = p^*$.

Thus, the system of seminorm LSTD- \bar{p}_t reduces to a single seminorm LSTD- p^* approximator, then to a (norm) LSTD- p^* in a recurrent MC (where $p^*(s) > 0, \forall s \in \mathcal{S}$) whenever Assumption 2.1 and a non-singularity condition about $(\mathbf{I} - \mathbf{P})$ are satisfied (see Sec 2). In such cases, the minimizer (17) becomes $\tilde{w}^* = (\mathbf{Z}^{-1/2} \mathbf{X})^{-1} \mathbf{Z}^{-1/2} \mathbf{y} = \mathbf{X}^{-1} \mathbf{Z}^{1/2} \mathbf{Z}^{-1/2} \mathbf{y} = \mathbf{X}^{-1} \mathbf{y} = \mathbf{w}^*$, which is (7).

Table 1: Unification of LSTD-based approximation methods by the general procedure (Def 4.4, the right-most column) for three types (rows) of environments (Envs). Here, $p_{\text{tr}}^{\#}$ denotes the transient part of $p^{\#}$ (20). This summary contains the representatives of existing average- and discounted-reward LSTD-based methods for the first and second types of environments.

Envs \ Methods	Norm LSTD- p^*	Norm LSTD- $p_{\text{tr}}^{\#}$	Seminorm LSTD- \bar{p}_t
Recurrent states only	Yu and Bertsekas (2009); Ueno et al. (2008)	Not applicable since recurrent state information is removed	One neighborhood $\mathcal{N}_{t=0}$ with $\bar{p}_0 = p^*$ (Fig 1: top row)
Multiple transient states and one 0-reward recurrent state	Not applicable since $p^*(s_{\text{tr}}) = 0$ for every transient state s_{tr} in \mathcal{S}_{tr}	Bradtke and Barto (1996); Boyan (2002)	Two neighborhoods: $\mathcal{N}_{t=0}$ and $\mathcal{N}_{t_{\text{abs}}^{\text{max}}}$ with $\bar{p}_0 = p^{\#}$, $\bar{p}_{t_{\text{abs}}^{\text{max}}} = p^*$ (Fig 1: second row)
Multiple transient states and multiple recurrent states	Not applicable (same as middle row)	Not applicable (same as top row)	At least two neighborhoods (Sec 5)

Second is the transient-state-only discounted-reward LSTD (Bradtke and Barto, 1996, Thm 1), which was designed for an MC with multiple transient states, plus a single known 0-reward absorbing terminal state (denoted as s_{zrat}). This is a special case of the general procedure (Def 4.4) when $n_a \leftarrow 2$, as illustrated in Fig 1: second-row. The first anchor is at $t = 0$ as always, whereas the second anchor is at the maximum absorption time $t = t_{\text{abs}}^{\text{max}}$, which is defined below.

Definition 4.5. Let \mathbf{P}_{tr} be a non-stochastic $|\mathcal{S}|-$ by- $|\mathcal{S}|$ matrix that is obtained by nullifying (setting to zero) the rows and columns corresponding to the recurrent states of the one-step transition matrix \mathbf{P} . Then, the maximum absorption time $t_{\text{abs}}^{\text{max}}$ is the time required by a Markov chain such that the $t_{\text{abs}}^{\text{max}}$ -th power of \mathbf{P}_{tr} is close to a zero matrix. That is,

$$t_{\text{abs}}^{\text{max}}(\varepsilon) := \min\{t : \|\mathbf{P}_{\text{tr}}^t\|_{\text{F}} \leq \varepsilon\}, \quad \text{and for an infinitesimally small } \varepsilon, \quad t_{\text{abs}}^{\text{max}} := t_{\text{abs}}^{\text{max}}(\varepsilon = 10^{-8}).$$

This $t_{\text{abs}}^{\text{max}}$ can be interpreted as the timestep at which there is (almost) no probability mass over all transient states for the first time. Such probability mass has moved to one or more recurrent states. Here, $\|\mathbf{P}_{\text{tr}}^t\|_{\text{F}}$ denotes the Frobenius matrix norm of \mathbf{P}_{tr}^t .

Setting the second anchor to $t_{\text{abs}}^{\text{max}}$ induces the following two desirable properties.

- i. The support of the first neighborhood \mathcal{N}_0 contains all transient states (as long as the initial state distribution allows), i.e. $\mathcal{S}_{\text{tr}} \subseteq \mathcal{S}(\bar{p}_0)$, where \mathcal{S}_{tr} denotes the transient state subset. This cannot be achieved by setting the second anchor to the minimum or the *expected* absorption time, by which some transient states may not be contained in $\mathcal{S}(\bar{p}_0)$. Note that since the absorption time is a random variable, it cannot be set as an anchor (Def 4.1).
- ii. The first neighborhood's state distribution \bar{p}_0 yields reasonable weighting for transient states in $\tilde{\mathcal{E}}_{\mathbb{P}\mathbb{B}}$ (4). It is reasonable in that \bar{p}_0 reflects the frequencies of visiting transient states before absorption. This is in contrast to, for example, setting the second anchor to $t = 1$ whenever the initial state distribution \hat{p} is uniform over \mathcal{S}_{tr} . It induces Property i. above as $\mathcal{S}_{\text{tr}} = \mathcal{S}(\bar{p}_0 \leftarrow \hat{p})$, but does not reflect transient state visitation since transient states may be visited beyond the first timestep (till absorption).

For an MC with multiple transient states and a known s_{zrat} (which is recurrent), the first neighborhood's state distribution \bar{p}_0 can be modified such that the probability mass is completely concentrated over \mathcal{S}_{tr} . Let $p^{\#}$ be the modified \bar{p}_0 and $t_{\text{abs}}^{\text{max}}$ be the maximum absorption time (Def 4.5). Then,

$$(p^{\#})^{\text{T}} = \hat{p}^{\text{T}} \left[\frac{1}{t_{\text{abs}}^{\text{max}}} \sum_{t=0}^{t_{\text{abs}}^{\text{max}}-1} \mathbf{P}_{\text{tr}}^t \right] = \hat{p}^{\text{T}} \left[\frac{1}{t_{\text{abs}}^{\text{max}}} \left\{ \underbrace{(\mathbf{I} - \mathbf{P}_{\text{tr}})^{-1}}_{\sum_{t=0}^{\infty} \mathbf{P}_{\text{tr}}^t} - \sum_{t=t_{\text{abs}}^{\text{max}}}^{\infty} \mathbf{P}_{\text{tr}}^t \right\} \right], \quad (20)$$

which is then normalized to $p^{\#} \leftarrow p^{\#} / \|p^{\#}\|_1$ to be a vector of probability values of $p^{\#}$. Here, $\sum_{t=t_{\text{abs}}^{\text{max}}}^{\infty} \mathbf{P}_{\text{tr}}^t$ is infinitesimally small by Def 4.5, whereas $(\mathbf{I} - \mathbf{P}_{\text{tr}})^{-1}$ is a non-stochastic $|\mathcal{S}|-$ by- $|\mathcal{S}|$

matrix whose $[s_0, s]$ -entry indicates the expected number of times the agent visits the state s , when it begins in the initial state s_0 (Grinstead and Snell, 2012, Thm 11.4).² Therefore, the state visitation from $t = 0$ (in a non-absorbing transient state) until absorption is mainly distributed according to $p^\#$.

Thus, the first approximator (of a system of two approximators anchored at $t = 0$ and $t_{\text{abs}}^{\text{max}}$) is devoted to estimating the value of transient states. It is originally a seminorm LSTD- $(\bar{p}_0 \leftarrow p^\#)$, but “forced” to become a norm variant by the following two ways (in addition to satisfying Assumption 2.1).

- The s_{zrat} entries in $p^\#, r, F,$ and P are removed. Such removal is possible because the state classification is known, namely the transient states are states that are visited before termination (i.e. before visiting the only recurrent s_{zrat}). It is also justifiable because there is no need to estimate the value of s_{zrat} , which is known to be zero (due to a zero reward).
- All transient states in \mathcal{S}_{tr} have positive probabilities in $p^\#$. This is guaranteed for example, whenever the support of the initial state distribution \hat{p} contains the whole \mathcal{S}_{tr} . Otherwise, a certain transition structure is needed such that $p^\#(s) > 0, \forall s \in \mathcal{S}_{\text{tr}}$.

The second and the last approximator, i.e. a seminorm LSTD- $(\bar{p}_{t_{\text{abs}}^{\text{max}}} \leftarrow p^*)$, concerns with estimating the value of the only recurrent state s_{zrat} . As a result, it is never needed because the value of s_{zrat} is known to be zero to the agent operating in an MC with a single 0-reward absorbing terminal state. Note that the last neighborhood’s state distribution is the stationary distribution p^* (as always), which is the limit of the lumpsum state distribution (Def 4.2) as t goes to infinity (from $t = t_{\text{abs}}^{\text{max}}$).

4.2 Potential benefits with more than two neighborhoods

One extreme of the general procedure (Def 4.4) is to specify as many neighborhoods as timesteps, as illustrated in Fig 1: bottom-row. This implies one seminorm LSTD- $(\bar{p}_t \leftarrow p^t)$ approximator for each timestep, where \bar{p}_t takes its specific form of p^t since there is merely an anchor (without any neighbor) in every neighborhood \mathcal{N}_t . At first, such stepwise treatment may seem as an overkill for a time-homogenous MDP with two state types. It is however, beneficial in three folds as follows.

First, each stepwise LSTD- p^t approximator is fed with independent and identically distributed (i.i.d) samples drawn from the corresponding stepwise state distribution p^t across multiple independent trials (see Algo 1). This is in contrast to samples from a lumpsum state distribution \bar{p}_t in a neighborhood with one or multiple neighbors. Those drawn from such \bar{p}_t in the same trial are Markovian samples, which yield biased sample means for $X, Z,$ and y for the LSTD- p^t minimizer in Thm 3.1.

Second, the stepwise distribution may have a support smaller than the whole state set, that is $|\mathcal{S}(p^t)| < |\mathcal{S}|$. The stepwise approximator’s generalization therefore can be focussed on fewer states, rather than all states in \mathcal{S} . By product, a system of stepwise LSTD- p^t also enables stepwise trade-off between approximation accuracy and capacity (which is limited due to e.g. the number of parameters).

Third, putting computation cost aside, stepwise treatment is a way to deal with unknown state classification in model-free RL by exploiting what the agent knows, that is the timestep t along with the corresponding state and reward samples at t . This is crucial for unichain MDPs with multiple transient states and multiple recurrent states. In addition, the unichain category includes recurrent MDPs and those with transient states and one recurrent state (as in Table 1). Because of this generality therefore, the unichain category should be used to model an environment for which we are not sure about its MDP classification (and are not willing to make some restrictive assumption).

We propose a resolution to the scalability issue of stepwise LSTD- p^t in the next Sec 4.3. It accommodates the use-case of more than two but much less than many neighborhoods (required by the stepwise extreme). This is at the cost of getting a reduced amount of the above-mentioned benefits.

4.3 Parsimoniously specifying the number of neighborhoods

The very first step of the general procedure (Def 4.4) is neighborhood specification. It amounts to locating n_a anchor timesteps along the whole time-horizon (see Fig 1). As discussed in Secs 4.1 and 4.2, the initial timestep $t = 0$ always serves as the first anchor. For $n_a = 2$, the second anchor is at

²Grinstead and Snell (2012, Thm 11.3) proved that $\lim_{t \rightarrow \infty} P_{\text{tr}}^t = \mathbf{0}$, suggesting that P_{tr} is generally not nilpotent. However, for some MCs (e.g. those with deterministic transition), P_{tr} is a nilpotent matrix whose degree is equal to $t_{\text{abs}}^{\text{max}} \leq |\mathcal{S}_{\text{tr}}|$.

$t = t_{\text{abs}}^{\max}$ (whenever t_{abs}^{\max} is known to the agent). Afterwards, the anchor locations are obvious only for $n_a = \infty$, by which every timestep is an anchor.

It is desirable to be able to locate a finite number of anchors, i.e. $2 \leq n_a < \infty$, in the context of model-free RL for unichain MDPs where the state classification (hence, the t_{abs}^{\max}) is unknown. Therefore, we aim to balance the advantage of having more anchors (Sec 4.2) and the computation of the required seminorm LSTD approximators. The latter can be indicated by the number of learnable parameters per approximator, that is $\dim(\mathbf{w}) < |\mathcal{S}|$. Moreover, a stricter computation budget limits the overall number of parameters in the system of n_a approximators. That is,

$$\{\dim(\mathbf{w}) \cdot n_a\} < |\mathcal{S}| \iff \left\{ \rho := \frac{\dim(\mathbf{w})}{|\mathcal{S}|} \right\} < \frac{1}{n_a} \iff n_a < \left\{ \frac{|\mathcal{S}|}{\dim(\mathbf{w})} = \frac{1}{\rho} \right\}, \quad (21)$$

where ρ indicates the numbers of parameters (per approximator) to states proportion, and $\dim(\mathbf{w})$ is equal to the number of feature dimensions in linear approximators. The above inequalities come from the motivation of using weighted error functions: trading-off approximation accuracy across states whenever the number of learnable parameters, $\dim(\mathbf{w})$, is (much) less than the number of states, $|\mathcal{S}|$.

For parsimoniously specifying timestep neighborhoods, we propose restricting neighbors' state distribution to be *in average*, within a tolerance distance Δ from their anchors'. This is an attempt to resemble one state distribution per neighborhood (so that states sampled from such a neighborhood's distribution are identically distributed) as much as Δ allows. Setting $\Delta \leftarrow 0$ yields one anchor per timestep (till the mixing time), whereas $\Delta \leftarrow \infty$ trivially yields one anchor at $t = 0$. Consequently, the effective range is at $0 < \Delta < \infty$, where Δ is also anticipated to be greater than the threshold used for determining whether the MC process has been mixing. For a desired n_a anchors, the tolerance Δ ideally puts the last anchor close and after the unknown t_{abs}^{\max} so that the preceding $(n_a - 1)$ approximators are mostly for estimating transient state values (whereas the last is for recurrent state values, as always). It is reasonable to have more anchors at the outset, during which the stepwise state distributions p^t are likely to be non-stationary (time-variant).

Our proposal above relies on the distance between two unknown state distributions, namely the anchor's p^t and the candidate neighbor's $p^{t+\tau}$.³ We identify the following properties for determining the proper distance metric. **First**, the distance should be approximated based on two sets of i.i.d samples, without estimating the distribution directly (e.g. via empirical probabilities). This precludes the use of the total-variation and the earth mover distance since generally they require distribution estimations as an intermediate step. **Second**, the supports of those two distributions are likely to be different, even disjoint. This renders the Kullback–Leibler divergence inapplicable.

Based on the aforementioned properties, we choose the maximum mean discrepancy (MMD) (Gretton et al., 2012) as the distribution distance metric. It relies on mapping the state distribution p^t into their so-called mean embedding μ_{p^t} . That is,

$$\mu : \mathcal{P}_{\mathcal{S}} \mapsto \mathcal{H}_k, \quad (22)$$

$$p^t \mapsto \mu_{p^t} := \sum_{s \in \mathcal{S}} p^t(s) k(s, \cdot) = \mathbb{E}_{S \sim p^t} [k(S, \cdot)], \quad (23)$$

where $\mathcal{P}_{\mathcal{S}}$ denotes the space of probability distributions over \mathcal{S} , and \mathcal{H}_k the reproducing kernel Hilbert space, which is induced by a positive definite kernel $k : \mathcal{S} \times \mathcal{S} \mapsto \mathbb{R}$. Here, \mathcal{H}_k is a space of functions mapping \mathcal{S} into \mathbb{R} . That is,

$$\begin{aligned} \phi : \mathcal{S} &\mapsto \mathcal{H}_k, & (\mathcal{H}_k = \text{span}\{k(s, \cdot) | s \in \mathcal{S}\}) \\ s &\mapsto \phi(s) := \phi(s)(\cdot) = k(s, \cdot), & \text{(Compare with (23), where the mean of } k(S, \cdot) \text{ is taken)} \end{aligned}$$

where $\phi(s) := \phi(s)(\cdot)$ denotes a function that assigns the value $k(s, s') \in \mathbb{R}$ to any $s' \in \mathcal{S}$.

³One alternative is the distribution ratio of $p^{t+\tau}/p^t$. However, density-ratio estimation typically requires another set of learnable parameters (Sugiyama et al., 2012). Moreover, our use-case involves many such ratios.

The MMD is an instance of an integral probability metric, whose supremum is over functions ψ in the unit ball of \mathcal{H}_k . Such MMD, denoted by $M_{\mathcal{H}_k}$, is formulated by [Gretton et al. \(2012\)](#) as

$$\begin{aligned}
M_{\mathcal{H}_k}^2(p^t, p^{t+\tau}) &:= \left[\sup_{\|\psi\| \leq 1} \left\{ \sum p^t(s)\psi(s) - \sum p^{t+\tau}(s)\psi(s) \right\} \right]^2 = \left[\sup_{\|\psi\| \leq 1} \{ \langle \psi, \mu_{p^t} - \mu_{p^{t+\tau}} \rangle \} \right]^2 \\
&= \|\mu_{p^t} - \mu_{p^{t+\tau}}\|_{\mathcal{H}_k}^2 = \langle \mu_{p^t}, \mu_{p^t} \rangle_{\mathcal{H}_k} + \langle \mu_{p^{t+\tau}}, \mu_{p^{t+\tau}} \rangle_{\mathcal{H}_k} - 2\langle \mu_{p^t}, \mu_{p^{t+\tau}} \rangle_{\mathcal{H}_k} \\
&= \mathbb{E} \left[\langle \phi(S_t), \phi(\acute{S}_t) \rangle_{\mathcal{H}_k} \right] + \mathbb{E} \left[\langle \phi(S_{t+\tau}), \phi(\acute{S}_{t+\tau}) \rangle_{\mathcal{H}_k} \right] - 2\mathbb{E} \left[\langle \phi(S_t), \phi(S_{t+\tau}) \rangle_{\mathcal{H}_k} \right] \\
&= \mathbb{E} \left[k(S_t, \acute{S}_t) \right] + \mathbb{E} \left[k(S_{t+\tau}, \acute{S}_{t+\tau}) \right] - 2\mathbb{E} \left[k(S_t, S_{t+\tau}) \right] \\
&\approx \frac{2}{n_{\text{exp}}} \sum_{i=1}^{n_{\text{exp}}/2} k(s_t^{2i-1}, s_t^{2i}) + k(s_{t+\tau}^{2i-1}, s_{t+\tau}^{2i}) - k(s_t^{2i-1}, s_{t+\tau}^{2i}) - k(s_t^{2i}, s_{t+\tau}^{2i-1}),
\end{aligned} \tag{24}$$

where n_{exp} denotes the number of experiment-episodes (trials), and s_t^i the state sample at timestep t in the i -th trial. The last expression is an unbiased estimator (of the *squared* MMD) that can be computed in linear time, and may be negative ([Gretton et al., 2012](#), Lemma 14). Note that state samples from the same i -th trial are not used in such estimation in (24).

To become a metric (instead of a pseudo-metric), MMD requires characteristic kernels, which subsumes universal kernels. This ensures that each distribution maps to a unique mean embedding in \mathcal{H}_k (i.e. μ_{p^t} in (22) is injective, thus characterizes the distribution p^t). Ideally, we have such a kernel that operates in the original state representation, which may not be in a Euclidean space. For discrete states, one example is the identity (Dirac) kernel, namely $k(s, s') := \mathbb{I}[s = s']$, whenever the identity operator \mathbb{I} is available to the agent. It induces a positive definite kernel Gram matrix, hence a *strictly* positive definite kernel that is always universal on discrete domains ([Muandet et al., 2017](#), p42). We note that converting a state distance (e.g. based on the bisimulation metric ([Ferns et al., 2006](#))) into a kernel Gram matrix is likely to yield a kernel that is not even positive definite, unless it satisfies certain conditions ([Haasdonk and Bahlmann, 2004](#)).

In some cases, discrete states are represented as numerical feature vectors in a Euclidean space. They are obtained via a state feature function $\mathbf{f}(s) \in \mathbb{Z}^{\dim(w)}$ (e.g. one-hot encoding), or $\mathbf{f}(s) \in \mathbb{R}^{\dim(w)}$. For these, one popular choice is the Gaussian radial-basis-function (RBF) kernel, namely

$$k(\mathbf{f}(s), \mathbf{f}(s')) := \exp\left(-\frac{\|\mathbf{f}(s) - \mathbf{f}(s')\|_2^2}{2\sigma^2}\right), \quad \text{with a width (length-scale) hyperparameter } \sigma, \tag{25}$$

which is a universal kernel on compact domains ([Muandet et al., 2017](#), Table 3.1). This kernel is relatively interpretable in that it involves a squared Euclidean distance between $\mathbf{f}(s)$ and $\mathbf{f}(s')$ scaled by the width hyperparameter σ . A very small σ yields a kernel matrix that is close to an identity matrix, implying every state is different. On the other hand, a very large σ yields a kernel matrix whose entries are all close to 1, implying all states are the same. Some RL works use this kernel for discrete state environments, e.g. [Song et al. \(2016\)](#); [Grünwälder et al. \(2012\)](#); [Xu et al. \(2005\)](#).

5 Approximating the bias of transient and recurrent states

In this section, we describe our proposed approach to approximating the bias values of unichain MDPs in model-free RL settings. It is devised from the general procedure (Sec 4) with two additional components specific to bias computation. They are about reference states and offsets, presented in Sec 5.1. Subsequently, we explain our proposed pseudocode in Sec 5.2. Its entry point is Algo 1, which is about training (learning) the estimator in model-free RL settings.

5.1 Reference states and offset calibration

As explained in Sec 2, the projected Bellman error \tilde{e}_{PB} (4) is derived from the average-reward evaluation equation (3) for unichain MDPs. The equation is re-written below, where the bias state value is denoted as b , instead of v (from now on, v denotes the *relative* bias state value).

$$\tilde{\mathbf{b}} = \mathbf{r} - \tilde{\mathbf{g}}\mathbf{1} + \mathbf{P}\tilde{\mathbf{b}} \iff (\mathbf{I} - \mathbf{P})\tilde{\mathbf{b}} = \mathbf{r} - \tilde{\mathbf{g}}\mathbf{1}, \quad (\text{An underdetermined linear system}) \tag{26}$$

whose solutions are $\tilde{g} = g$, and $\tilde{\mathbf{b}} = \mathbf{b} + o\mathbf{1}$, where g is the scalar gain (which is constant across states in unichain MDPs), $\mathbf{b} \in \mathbb{R}^{|\mathcal{S}|}$ is the bias vector, and $o \in \mathbb{R}$ is an arbitrary offset (Puterman, 1994, Corollary 8.2.7).⁴ To obtain a solution for $\tilde{\mathbf{b}}$ in (26) that is unique (but not necessarily equal to \mathbf{b}), we set the arbitrary offset to a certain value, e.g. $o \leftarrow -\tilde{b}(s_{\text{ref}})$ for an arbitrary reference state s_{ref} . This yields $\tilde{\mathbf{b}} \leftarrow \tilde{\mathbf{b}} - \tilde{b}(s_{\text{ref}})\mathbf{1}$, whose resulting value is called the *relative* bias value at s_{ref} .

Thus, the bias approximation (by minimizing \tilde{e}_{PB}) actually estimates the relative bias value \mathbf{v} , which is equal to the bias \mathbf{b} up to some offset o . That is, $\hat{\mathbf{v}} \approx \{\mathbf{v} = \mathbf{b} + o\mathbf{1}\}$. Since any arbitrary offset satisfies (26), we can adjust the offset o to be $o \leftarrow -b(s_{\text{ref}})$ in a similar fashion as determining a unique $\tilde{\mathbf{b}}$ (in the previous passage). This is somewhat advantageous since at least, one true relative-value at s_{ref} is known to be zero, namely $v(s_{\text{ref}}) = b(s_{\text{ref}}) + \{o = -b(s_{\text{ref}})\} = 0$. Therefore, we introduce a *prediction* offset, denoted as \tilde{o} , and set it to $\tilde{o} \leftarrow -\hat{v}(s_{\text{ref}})$ in order to ensure that the predicted relative value at s_{ref} matches with its true value. That is, $\hat{\mathbf{v}} \leftarrow \hat{\mathbf{v}} + \tilde{o}\mathbf{1}$ such that $\hat{v}(s_{\text{ref}}) = \hat{v}(s_{\text{ref}}) + \{\tilde{o} = -\hat{v}(s_{\text{ref}})\} = v(s_{\text{ref}}) = 0$.

Adjusting the prediction of multiple approximators requires a bit of work, which we explain in the rest of this section. They are about identifying reference states and calibrating prediction offsets.

5.1.1 Identifying reference states in a system of multiple approximators

For a system of approximators of the general procedure (Def 4.4), one strategic choice for s_{ref} is the most common state across all neighborhood supports (Def 4.2) with a tie-breaking rule as in Def 5.1. This s_{ref} is deemed as the *main* reference state of the system. Note that s_{ref} is not necessarily a recurrent state due to neighborhood specification and in practice, because there is a finite number of timesteps and the neighborhood supports are estimated based on empirical state samples.

Definition 5.1. *When determining the most common states across multiple neighborhood supports, any tie (including when the state frequencies are all ones) is resolved by selecting any state from the earliest neighborhood for prioritizing the estimation accuracy of transient state values.*

For the remaining neighborhoods whose supports do not contain the main s_{ref} , we search for potentially multiple auxiliary reference states s'_{ref} via the following procedure.

1. Initialize the reference state set $\mathcal{S}_{\text{ref}} \leftarrow \{s_{\text{ref}}\}$.
2. Search for an auxiliary reference state s'_{ref} that simultaneously satisfies two rules below,
 - i. the most common among neighborhood supports that are disjoint with \mathcal{S}_{ref} (using the same tie-breaking as for identifying the main s_{ref} (Def 5.1)), and
 - ii. contained in any neighborhood support that is not disjoint with \mathcal{S}_{ref} .
3. If a new auxiliary s'_{ref} is found and there is at least one neighborhood that still does not have any reference state, then $\mathcal{S}_{\text{ref}} \leftarrow \mathcal{S}_{\text{ref}} \cup \{s'_{\text{ref}}\}$ and go to Step 2. Otherwise, stop.

After applying the above procedure, there may exist neighborhoods whose supports still do not contain either the main s_{ref} or any auxiliary s'_{ref} .⁵ Such neighborhoods are eventually merged to their nearest (in terms of timesteps) neighborhood with any type of reference states (the precedence is given to the preceding neighborhood whenever tie occurs). The earliest anchor (among those of the merged neighborhoods) becomes the anchor of the newly-formed neighborhood, whereas the other (now defunct) anchors become the neighbors.

5.1.2 Calibrating prediction offsets in a system of multiple approximators

Once every neighborhood \mathcal{N}_t (whose approximator is denoted by \hat{v}_t) is assigned a reference state, its prediction offset \tilde{o}_t is set as follows.

$$\tilde{o}_t \leftarrow -\hat{v}_t(s_{\text{ref}}), \quad \text{for each approximator } \hat{v}_t \text{ with the main } s_{\text{ref}}, \text{ and} \quad (27)$$

$$\tilde{o}_{t'} \leftarrow [\hat{v}_t(s'_{\text{ref}}) + \tilde{o}_t] - \hat{v}_{t'}(s'_{\text{ref}}), \quad \text{for each approximator } \hat{v}_{t'} \text{ with an auxiliary } s'_{\text{ref}} \quad (28)$$

⁴Another equation, i.e. $\mathbf{P}^*\tilde{\mathbf{b}} = \mathbf{0}$, is required to be able to determine $\tilde{g} = g$, and $\tilde{\mathbf{b}} = \mathbf{b}$ uniquely without any offset. Note that plugging the true gain (e.g. from $g = (\mathbf{p}^*)^\top \mathbf{r}$) to (26) does not change the situation in that (26) still admits multiple solutions (even though the issue of underdetermination has been remedied). This is because (26) involves a singular matrix $(\mathbf{I} - \mathbf{P})$.

⁵We conjecture that in theory, an auxiliary s'_{ref} exists for every neighborhood whenever at least one of the following conditions is fulfilled, namely i) each state has non-zero probabilities for transitioning to itself, as well as for transitioning to another state, and ii) the initial state distribution $\tilde{\mathbf{p}}$ has the whole state set as its support.

where \hat{v}_t in (28) is of any neighborhood whose support contains s'_{ref} . These \tilde{o}_t are then applied to the corresponding prediction as $\hat{v}_t \leftarrow \hat{v}_t + \tilde{o}_t \mathbf{1}$. Algo 5 implements this prediction calibration.

Applying the prediction offset \tilde{o} to a system of approximators forces at least one state to have the same approximated value in two neighborhoods.⁶ This is the cost we pay for two purposes. **First** is to propagate the unique and true relative bias value at the main reference state s_{ref} , namely $\hat{v}(s_{\text{ref}}) = v(s_{\text{ref}}) = 0$, throughout all neighborhoods' approximators. This propagation is carried out exactly for neighborhoods with the main reference state s_{ref} via (27). For those with an auxiliary reference state s'_{ref} , it is carried out approximately via (28). **Second** is to accommodate the joint-use of multiple relative-value approximators, which originally have different offsets with respect to the true bias. Such a use-case arises for example, when computing a quantity that involves relative values of multiple transient and recurrent states whose estimates come from multiple approximators.

5.2 Pseudocode

In this section, we present the pseudocode for the proposed relative-value approximator from multiple transient and recurrent states. The central pseudocode is Algo 1, which contains the training protocol in model-free RL settings. After obtaining state and reward samples, it specifies a list of neighborhoods (Algo 2), computes the minimizer of the seminorm LSTD for each neighborhood (Sec 3.2), and finally calibrates the prediction offset (Algo 5).

Specifically, Algo 2 approximates the timestep locations of anchors (via Algo 3), then identifies the anchors' reference states (via Algo 4). Algo 3 relies on MMD to measure the distributional distance between each anchor and its neighbor candidates (Sec 4.3). For an anchor at timestep t , one may select (or sample) a reasonable number of timesteps from a set $\{t + 1, t + 2, \dots, \hat{t}_{\text{max}}^{\text{ep}}\}$ as neighbor candidates, for which their state distribution distances from the anchor's are approximated.

Algorithm 1: Training a system of relative-value approximators for transient and recurrent states in model-free settings. This implements the general procedure (Def 4.4).

Input: A stationary policy π , a state feature function \mathbf{f} , a kernel function k , a number of anchors n_a , a number of experiment-episodes (trials) n_{xep} (each is with $\hat{t}_{\text{max}}^{\text{ep}} + 1$ timesteps).

Output: A list of neighborhoods $\tilde{\mathcal{N}}$ along with their parameters $\tilde{\mathcal{W}}$ and prediction offsets $\tilde{\mathcal{O}}$.

```

1 Initialize stepwise state and reward lists of sample lists:  $\tilde{\mathcal{S}} \leftarrow \emptyset$  and  $\tilde{\mathcal{R}} \leftarrow \emptyset$ , respectively.
2 for Each experiment-episode (trial)  $i = 0, 1, \dots, n_{\text{xep}} - 1$  do
3   Reset the environment, and obtain an initial state  $s_0$ , then set the state variable  $s \leftarrow s_0$ .
4   for Each timestep  $t = 0, 1, \dots, \hat{t}_{\text{max}}^{\text{ep}}$  do
5     Choose to then execute an action  $a$  based on  $\pi(\cdot|s)$ .
6     Observe the next state  $s'$  and the reward  $r$ .
7     Append samples  $s$  and  $r$  to the corresponding  $\tilde{\mathcal{S}}$  and  $\tilde{\mathcal{R}}$  at index  $t$ .
8     Update the current state variable  $s \leftarrow s'$ .
9   if Desired (at least once) then
10     Get a list of neighborhoods,  $\tilde{\mathcal{N}} \leftarrow \text{SpecifyNeighborhoods}(\tilde{\mathcal{S}}, n_a, k)$ . ▷ Algo 2
11     Set an empty list of learned weights  $\tilde{\mathcal{W}} \leftarrow \emptyset$ .
12     for Each neighborhood  $\mathcal{N}_t \in \tilde{\mathcal{N}}$  do
13       Learn the minimizing parameter  $\tilde{w}_t$  using  $\mathcal{N}_t, \tilde{\mathcal{S}}, \tilde{\mathcal{R}}$ , and  $\mathbf{f}$ . ▷ Thm 3.1
14       Put this learned  $\tilde{w}_t$  to  $\tilde{\mathcal{W}}$  at index  $t$ .
15     Calibrate the prediction offsets,  $\tilde{\mathcal{O}} \leftarrow \text{CalibrateOffset}(\tilde{\mathcal{W}}, \tilde{\mathcal{N}}, \mathbf{f})$ . ▷ Algo 5
16 return  $\tilde{\mathcal{N}}, \tilde{\mathcal{W}}$ , and  $\tilde{\mathcal{O}}$ .

```

⁶Recall that if (26), from which $\tilde{c}_{\mathbb{P}\mathbb{B}}$ is derived, did not admit multiple solutions, neighborhood-wise approximators would allow different value estimates for all states in different neighborhoods (Sec 4.2).

Algorithm 2: SpecifyNeighborhoods($\tilde{\mathcal{S}}, n_a, k$) specifies the timestep neighborhoods (Def 4.1).

Input: A state sample list $\tilde{\mathcal{S}}$, a desired number of anchors $n_a \geq 2$, and a kernel function k .

Output: A list of neighborhoods $\tilde{\mathcal{N}}$, each is augmented with reference state information.

```

1 Initialize a list of anchors,  $\tilde{\mathcal{T}} \leftarrow \emptyset$ .
2 if  $2 \leq n_a < \{\hat{t}_{\max}^{\text{exp}} = \text{length}(\tilde{\mathcal{S}}) - 1\}$  then
3    $\tilde{\mathcal{T}} \leftarrow \text{ApproximateAnchors}(\tilde{\mathcal{S}}, n_a, k)$ . ▷ Algo 3
4 else
5    $\tilde{\mathcal{T}} \leftarrow [0, 1, \dots, \hat{t}_{\max}^{\text{exp}}]$ . ▷ Stepwise anchors
6 Construct a neighborhood list  $\tilde{\mathcal{N}}$  based on  $\tilde{\mathcal{T}}$ . ▷ Def 4.1
7 Identify a reference state list,  $\mathcal{S}_{\text{ref}} \leftarrow \text{IdentifySref}(\tilde{\mathcal{N}}, \tilde{\mathcal{S}})$ . ▷ Algo 4
8 Retain or merge neighborhoods based on reference state existence in  $\mathcal{S}_{\text{ref}}$ . ▷ Sec 5.1.1
9 return  $\tilde{\mathcal{N}}$ .

```

Algorithm 3: ApproximateAnchors($\tilde{\mathcal{S}}, n_a, k$) approximates the anchor locations (Sec 4.3).

Input: A state sample list $\tilde{\mathcal{S}}$, a desired number of anchors $n_a \geq 2$, and a kernel function k .

Output: A list of anchors $\tilde{\mathcal{T}}$ (recall: an anchor is a timestep index).

```

1 Initialize the distance tolerance  $\Delta$  to a small positive number, and
  the current number of approximate anchors  $\bar{n}_a \leftarrow \hat{t}_{\max}^{\text{exp}}$  with  $\hat{t}_{\max}^{\text{exp}} = \text{length}(\tilde{\mathcal{S}}) - 1$ .
2 while  $\bar{n}_a > n_a$  do
3   Reset a list of anchors  $\tilde{\mathcal{T}} \leftarrow [0]$ , and the average neighbor-candidate distance  $\bar{\Delta}^2 \leftarrow 0$ .
4   for Each timestep  $t = 1, 2, \dots, \hat{t}_{\max}^{\text{exp}}$  do
5     Set the last anchor,  $\tilde{t} \leftarrow \tilde{\mathcal{T}}[-1]$ . ▷ The last item is at index -1
6     Get the squared MMD,  $\hat{d}_t^2$  by plugging-in state samples  $\tilde{\mathcal{S}}[t, \tilde{t}]$  and kernel  $k$  to (24).
7     Update  $\bar{\Delta}^2 \leftarrow \bar{\Delta}^2 + (\hat{d}_t^2 - \bar{\Delta}^2)/(t - \tilde{t})$ . ▷ Update the running average
8     if The average neighbor-candidate distance  $\bar{\Delta}^2 > \Delta^2$  then
9       Append  $t$  to the anchor list,  $\tilde{\mathcal{T}} \leftarrow \tilde{\mathcal{T}} + [t]$ .
10      Reset  $\bar{\Delta}^2 \leftarrow 0$ .
11   Update  $\bar{n}_a \leftarrow \text{length}(\tilde{\mathcal{T}})$ .
12   Increase the distance tolerance  $\Delta \leftarrow 2\Delta$ . ▷ For some multiplier, e.g. 2
13 return  $\tilde{\mathcal{T}}$ .

```

6 Experimental setup

In this section, we describe the setup of our experiments, whose results are presented in Sec 7. We begin with the environment specifications in Sec 6.1, followed by state features and state kernels (Sec 6.2). Then, various experiment schemes are described in Sec 6.3. Lastly, we explain the evaluation metrics and protocols in Sec 6.4.

6.1 Environments

We evaluate our proposed method on environments whose all stationary deterministic policies induce unichain MCs. Those environments are formed by connecting a recurrent MDP to a transient structure. Each environment is identified by a mnemonic, e.g. x123c, where the first letter (i.e. ‘x’) denotes a particular recurrent MDP, followed by a total number of states (i.e. ‘123’), and an identifier for the transient structure (i.e. ‘c’), which will be explained shortly.

We use the following recurrent MDPs from the literature. They are listed by their single-letter identifiers (which become the first letter in their environment mnemonics) as follows: ‘h’ is with 3 recurrent states (Hordijk et al., 1985), and ‘c’ is with 5 recurrent states (Strens, 2000). In these recurrent MDPs, every state has two available actions.

Algorithm 4: $\text{IdentifySref}(\tilde{\mathcal{N}}, \tilde{\mathcal{S}})$ identifies the neighborhoods' reference states (Sec 5.1.1).

Input: A list of neighborhoods $\tilde{\mathcal{N}}$ and a list of state samples $\tilde{\mathcal{S}}$.

Output: A list of reference states \mathcal{S}_{ref} .

```

1 Initialize lists of neighborhoods without reference states  $\hat{\mathcal{N}} \leftarrow \tilde{\mathcal{N}}$  and with reference states
   $\check{\mathcal{N}} \leftarrow \emptyset$ , and a list of reference states  $\mathcal{S}_{\text{ref}} \leftarrow \emptyset$  (which will contain  $s_{\text{ref}}$  of neighborhoods in
   $\hat{\mathcal{N}}$ ), and two variables: ForAuxSref to False and CandidateSrefIsValid to True.
2 while CandidateSrefIsValid and  $\hat{\mathcal{N}}$  is not empty do
3   Set  $\hat{\mathcal{S}}$  to the list of the supports of neighborhoods in  $\hat{\mathcal{N}}$ .
4   Set  $\check{\mathcal{S}}$  to the list of the supports of neighborhoods in  $\check{\mathcal{N}}$ .
5   Clear the list of banned  $s_{\text{ref}}$ , if any.  $\triangleright$  See the banning of  $s_{\text{ref}}$  in Line 9
6   for Each  $i = 1, 2, \dots$  until the number of unique states in  $\hat{\mathcal{S}}$  do
7     Set  $s_{\text{ref}}$  to the most-common unbanned support in  $\hat{\mathcal{S}}$  (with tie-breaking as in Def 5.1).
8     if ForAuxSref and ( $s_{\text{ref}}$  is not in  $\check{\mathcal{S}}$ ) then
9       Set CandidateSrefIsValid to False, ban this  $s_{\text{ref}}$ , and continue.
10    for Each neighborhood in  $\hat{\mathcal{N}}$  do
11      if  $s_{\text{ref}}$  is contained in the support of this neighborhood then
12        Set  $\hat{t}$  to this neighborhood's anchor.
13        Set  $\mathcal{S}_{\text{ref}}[\hat{t}] \leftarrow s_{\text{ref}}$ .  $\triangleright$  Either as a main or aux reference state
14        Remove this neighborhood from  $\hat{\mathcal{N}}$ , then add it to  $\check{\mathcal{N}}$ .
15      Set CandidateSrefIsValid to True, then break.
16    Set ForAuxSref to True.  $\triangleright$  Looking for the main  $s_{\text{ref}}$  is only in the 1st pass
17 return  $\mathcal{S}_{\text{ref}}$ .

```

Algorithm 5: $\text{CalibrateOffset}(\tilde{\mathcal{W}}, \tilde{\mathcal{N}}, \mathbf{f})$ calibrates the offsets of all approximators (Sec 5.1.2).

Input: Lists of learned parameters $\tilde{\mathcal{W}}$ and of neighborhoods $\tilde{\mathcal{N}}$, and a state feature function \mathbf{f} .

Output: A list of calibrated prediction offsets $\tilde{\mathcal{O}}$, which corresponds to $\tilde{\mathcal{W}}$.

```

1 Initialize a list of learned parameters (representing approximators) without calibrated offsets
   $\hat{\mathcal{W}} \leftarrow \tilde{\mathcal{W}}$ , as well as a list of calibrated prediction offsets  $\tilde{\mathcal{O}} \leftarrow \emptyset$ .
2 for Each neighborhood's anchor  $\tilde{t}$  with the main  $s_{\text{ref}}$  in  $\tilde{\mathcal{N}}$  do
3   Set  $\tilde{w}$  to the entry of  $\tilde{\mathcal{W}}$  at  $\tilde{t}$ , and remove the entry  $\tilde{w}$  from  $\hat{\mathcal{W}}$ .
4    $\tilde{\mathcal{O}}[\tilde{w}] \leftarrow -\mathbf{f}^\top(s_{\text{ref}}) \tilde{w}$ .  $\triangleright$  This implements (27)
5 while  $\hat{\mathcal{W}}$  is not empty do
6   Choose any entry  $\hat{w}$  in  $\hat{\mathcal{W}}$ .
7   Look up the auxiliary  $s'_{\text{ref}}$  of a neighborhood whose approximator is represented by  $\hat{w}$ .
8   for Each calibrated offset  $\tilde{o}$  in  $\tilde{\mathcal{O}}$  do
9     Set  $\tilde{w}$  to the learned parameter corresponding to  $\tilde{o}$ .
10    if  $s'_{\text{ref}}$  is in the support of a neighborhood whose approximator is represented by  $\tilde{w}$  then
11       $\tilde{\mathcal{O}}[\hat{w}] \leftarrow (\mathbf{f}^\top(s'_{\text{ref}}) \tilde{w} + \tilde{o}) - \mathbf{f}^\top(s'_{\text{ref}}) \hat{w}$ .  $\triangleright$  This implements (28)
12      Remove the entry  $\hat{w}$  from  $\hat{\mathcal{W}}$ , then break.
13 return  $\tilde{\mathcal{O}}$ .

```

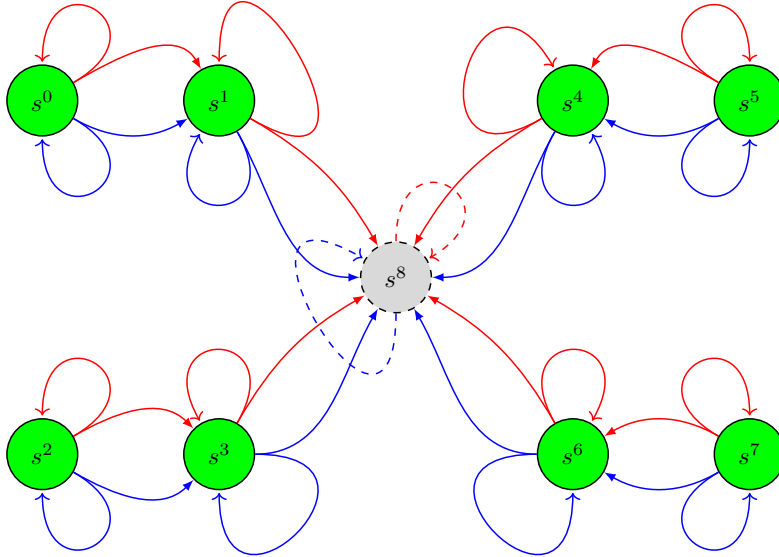


Figure 2: The diagram of an instance ‘x9d’ of generic unichain MDPs. In this instance, there are eight transient states (green solid circles) that belongs to four (labelled ‘d’) streams of transient states (here, each stream consists of two transient states). In every transient state, there are two available actions (red and blue solid edges), each has two possible outcomes: either the current state (self-loop) or another state. All four stream of transient states are connected to a recurrent MDP (labelled ‘x’), which has a single recurrent state (a gray dashed circle) with two self-loop actions (red and blue dashed edges). If there were multiple recurrent states, they would form a single recurrent class, which could be lumped together and represented by a single absorbing state in the diagram.

For transient structures, we use a generic structure as depicted in Fig 2. A specific instance of it is mainly characterized by the number of streams of transient states, for which multiple streams of 2, 3, . . . are denoted by a single letter of ‘b’, ‘c’, . . . , respectively (which becomes the last letter in the environment mnemonic). For simplicity, all streams have an identical transition and reward structure. They are also all connected to an arbitrary recurrent state. In all streams, every transient state has two available actions, where every action leads to two possible outcomes, namely its own state (self-loop, self-transition) and another state.

In these environments, the initial state is always transient. Specifically, the initial state distribution \hat{p} assigns a probability of $1/|\mathcal{S}_{\text{tr}}|$ for every transient state and 0 for every recurrent state.

6.2 State features and state kernels

Since feature extraction and selection are not the focus of this work, we use a random feature vector to represent a state. That is, the state feature $\mathbf{f}(s) \in \mathbb{R}^{\text{dim}(w)}$, $\forall s \in \mathcal{S}$, is constructed by randomly sampling each i -th dimension feature value as $f_i(s) \sim \mathcal{G}(\mu = \text{index}(s), \sigma^2 = 1)$, where \mathcal{G} is a Gaussian distribution with a mean μ (which is set to the non-negative integer index of a state s) and a unit variance σ^2 .

The aforementioned state features accomodates the use of Gaussian RBF kernels for computing the state-distribution distances using MMD (Sec 4.3). For experiments, we set the kernel width in (25) to 1 after the variance of the standard Gaussian distribution for $f_i(s)$.

6.3 Experiment schemes

Our experiment schemes are products of three sources of variations. **First** is the number of feature dimensions, indicated by the feature-to-state dimensional proportion ρ . Since we need at least two approximators (anchors) representing two states classes in unichain MDPs, the strict computation limit in (21) yields an upper bound of $\rho < 1/(n_a = 2)$. For experiments therefore, we select the following six feature dimension regimes, which in turn constraint the maximum number of anchors n_a^{\max} according to (21). They are collected as a set of tuples (ρ, n_a^{\max}) as follows,

$$\left\{ (0.49, \lfloor 2.04 \rfloor), (0.33, \lfloor 3.03 \rfloor), (0.19, \lfloor 5.3 \rfloor), (0.09, \lfloor 11.1 \rfloor), (0.06, \lfloor 16.7 \rfloor), (0.03, \lfloor 33.3 \rfloor) \right\}, \quad (29)$$

where $\lfloor x \rfloor$ indicates the flooring operation, i.e. the greatest integer less than or equal to x .

Second is based on algorithmic variations of the proposed method (Sec 5), as well as the baseline. Such variations come from varying the number of anchors⁷ and the state-distribution distance metrics. There are ten approximation schemes in four groups as follows.

- i. **‘buw’ and ‘p01’**: These mnemonics refer to the unweighted baseline and the proposed one-approximator scheme, respectively. The latter ‘p01’ has a single anchor at $t = 0$, and uses the seminorm LSTD because $\bar{p}_0 = p^*$ has only recurrent states as its support (hence, $\text{diag}(\bar{p}_0)$ is PSD). On the other hand, ‘buw’ uses a (norm) LSTD approximator because the state distribution is set to be uniform over all states. This uniformity also implies that the state-wise value errors are unweighted in $\tilde{e}_{\mathbb{P}\mathbb{B}}$ (4). We are not aware of any other baseline besides ‘buw’ for estimating the bias values from transient and recurrent states with parametric function approximators. Note that the existing methods are with a single norm LSTD, but they are applicable solely for recurrent MDPs (Yu and Bertsekas, 2009), or unichain MDPs with one zero-reward recurrent state (Bradtke and Barto, 1996).
- ii. **‘p02am’, ‘p02tv’, ‘p02ot’, and ‘p02md’**: These mnemonics refer to the proposed two-approximator schemes using various ways to determine the second anchor location, namely at a given maximum absorption time t_{abs}^{\max} (‘am’), or based on three different state-distribution distance metrics: total variation (TV, ‘tv’), optimal transport (OT, ‘ot’), and MMD (‘md’). The variant with t_{abs}^{\max} (‘p02am’) is instantiated so that the first neighborhood’s state distribution has all transient states in its support. It also matches the existing method for unichain MDPs with one 0-reward recurrent state (as explained in Sec 4.1). The variant with TV (‘p02tv’) is motivated by the fact that TV is a typical metric for determining the mixing time. We also experiment with an OT-based variant (‘p02ot’) because OT considers the state distance (as the underlying non-probabilistic metric)⁸, making it on par with the MMD variant (‘p02md’). Moreover, the neighborhood specification based on OT can serve as ground-truth whenever OT uses a state distance metric that does not depend on state representation (cf. MMD involves a state kernel whose hyperparameters are heuristically determined). For OT computation therefore, we use a behavioral state similarity derived from environment properties, such as transition and reward functions. It is the π -bisimulation pseudo-metric (Castro, 2020, Thm 2), specifically its state-action counterpart (Lan et al., 2021, Lemma 7). That is, the distance between two states s and s' under a policy π is given by $d_\pi(s, s') := \max_{a \in \mathcal{A}} |q_\gamma^\pi(s, a) - q_\gamma^\pi(s', a)|$, where q_γ^π is the discounted state-action value of π (here, the discount factor γ is set to 0.999).⁹ The variant ‘p02md’ relies on Algo 3 to determine the anchor locations based on the MMD metric.
- iii. **‘paxtv’, ‘paxot’, and ‘paxmd’**: These mnemonics refer to the proposed schemes with the maximum number of anchors n_a^{\max} (‘ax’) as allowed by the computation constraint (21) given the feature-to-state dimensional proportion ρ . Such n_a^{\max} values are specified in (29). The three variants here are due to different distribution distance metrics with the same justification as for ‘p02· ·’ in Item ii. above.
- iv. **‘pinf’**: This mnemonic refers to the proposed stepwise-approximator variant, where there are as many anchors as timesteps. In theory, there is an infinite number (‘inf’) of anchors since the horizon is infinite.

⁷Note that if some neighborhoods do not have joint supports, there will be fewer anchors than what is specified to Algo 1 and 2, as explained in Sec 5.1.1.

⁸We use the OT implementation of Flamary et al. (2021).

⁹To our knowledge, there is no behavioral state similarity metric for non-discounted rewards thus far.

Third is whether the experiments involve approximation due to sampling the initial state $S_0 \sim \hat{p}$ and the next state $S_{t+1} \sim p(\cdot|s_t, a_t)$, which affects the next reward $R_{t+1} := r(s_t, a_t, s_{t+1})$ for a deterministic reward function $r(\cdot)$ given s_t , a_t , and s_{t+1} . This leads to two kinds of experiments, namely sampling and non-sampling. Both share the following common properties (which are feasible to obtain for environments described in Sec 6.1).

- The exact gain of a policy is used so that the effect of our proposed method can be isolated.
- Each experiment-episode (trial) is run long enough in order to well approximate the infinite-horizon MDP model. The maximum timestep in each experiment-episode is set to a multiple of the mixing time, i.e. $\hat{t}_{\max}^{\text{exp}} \leftarrow 10t_{\text{mix}}$. Here, t_{mix} is exactly computed with high precision.

In sampling experiments, the scheme ‘buw’ is not feasible because a model-free RL agent generally cannot sample the states uniformly during the whole interaction with its environment. The same goes to the scheme ‘p02am’ in that t_{abs}^{\max} is unknown to the agent. The schemes involving TV and OT (i.e. ‘p·tv’, ‘p·ot’) also cannot be conducted in sampling experiments since they require constructing intermediate empirical probabilities based on samples (Sec 4.3).

6.4 Experimental evaluation metrics and protocols

The training of a system of approximators is as follows. We select one policy uniformly at random from the set of all stationary deterministic policies, and sample the random feature values as specified in Sec 6.2. Then, we run multiple n_{exp} independent experiment-episodes (trials), each is with $\hat{t}_{\max}^{\text{exp}} + 1$ timesteps, as prescribed in Algo 1. This training procedure is carried out for each environment and each approximation scheme (Sec 6.3).

The quality of a system of approximators is indicated by the accumulative total error of the square roots of stepwise errors along one evaluation experiment-episode. That is,

$$\varepsilon_x := \sum_{t=0}^{\hat{t}_{\max}^{\text{exp}}} \sqrt{e_x^t(\mathbf{w}_t)}, \quad \text{where } x \text{ is either } \mathbb{PB} \text{ or MS, and } \mathbf{w}_t \text{ is of the neighborhood to which } t \text{ belongs.} \quad (30)$$

We perform evaluations using both stepwise $e_{\mathbb{PB}}^t$ and e_{MS}^t , which utilize the stepwise state distribution p^t to weight state-wise errors as in (4) and (11), respectively. In particular, the exact p^t is used so that there is no sampling-error in evaluation (hence, one experiment-episode is sufficient for evaluation).

The use of $e_{\mathbb{PB}}^t$ and e_{MS}^t in (30) yields two evaluation metrics, i.e. $\varepsilon_{\mathbb{PB}}$ and ε_{MS} . The former $\varepsilon_{\mathbb{PB}}$ serves as the gold standard since $e_{\mathbb{PB}}^t$ is what the stepwise approximator (‘pinf’) minimizes. The $\varepsilon_{\mathbb{PB}}$ value is computed by plugging-in the learned (trained) parameter \mathbf{w}_t into the $\tilde{e}_{\mathbb{PB}}$ formula (4) with $\tilde{p} \leftarrow p^t$. On the other hand, the latter ε_{MS} is natural whenever the true value is known (but is never told to the RL agent) as for the environments described in Sec 6.1. For this, we predict the value of every state at every timestep t using \mathbf{w}_t , apply the prediction offset, i.e. $\hat{v}(s) \leftarrow \mathbf{w}_t^\top \mathbf{f}(s) + o_t$, then plug-in the predicted value $\hat{v}(s)$ to \tilde{e}_{MS} formula (11) weighted by $\tilde{p} \leftarrow p^t$.

7 Experimental results

In this section, we present the experimental results, whose setup is described in the previous Sec 6. There are two groups of results, namely non-sampling and sampling experiments, as explained in Sec 6.3. Each is evaluated with two error metrics, namely $\varepsilon_{\mathbb{PB}}$ and ε_{MS} (Sec 6.4).

7.1 Non-sampling experimental results

Tables 2 to 7 present the non-sampling results of ten schemes in six feature-to-state dimensional ratios (Sec 6.3) and six environments, modelled as unichain MDPs with transient states (Sec 6.1).

From the $\varepsilon_{\mathbb{PB}}$ standpoint, the results are as anticipated in that the lowest error is from the stepwise approximator (pinf), whereas the second and third lowests are from the maximum number of approximators (pax·) allowed by the feature-to-state dimensional ratios. More specifically, those with MMD (paxmd) are on par with OT (paxot) in most cases, where occasionally those with TV (paxtv) become either the second or third lowest errors (in lieu of paxmd or paxot).

The advantage of having multiple approximators is also obvious based on ε_{PB} , especially as the dimensional ratio ρ decreases. Those with a single approximator (i.e. buw and p01) have up to 100-fold larger errors than those with two approximators (p02· ·). The similar behaviour is also observed between ‘p02· ·’ and those with even more approximators, i.e. ‘pax· ·’. Among two-approximator schemes, those with a given $t_{\text{abs}}^{\text{max}}$ (p02am) do not necessarily yield the lowest ε_{PB} . This is because the first approximator of p02am may not estimate the values of the least number of recurrent states, compared to p02tv, p02ot, and p02md. Recall that for ‘p02· ·’, the first approximator should be devoted, as much as possible, to estimating transient states. Some recurrent states however, may already have non-zero probabilities before $t_{\text{abs}}^{\text{max}}$.

From the ε_{MS} standpoint, the stepwise approximator (pinf) achieves the lowest value or at least, the second lowest in some environments. This is a direct result of obtaining small ε_{PB} . In contrast, the other approximator schemes do not achieve small ε_{PB} . As a consequence, their ε_{PB} do not correlate with their ε_{MS} counterparts. That is, lower ε_{PB} do not necessarily mean lower ε_{MS} . This phenomenon is also observed by [Dann et al. \(2014, Sec 3.2.2\)](#). Recall that directly minimizing ε_{MS} is not possible in RL since it requires the knowledge of true (ground-truth) state values as in (11).

Interestingly, the second lowest ε_{MS} is achieved by the two-approximator scheme with a given $t_{\text{abs}}^{\text{max}}$ (i.e. p02am) in most cases; otherwise, p02am achieves even better results as the lowest. The third lowest ε_{MS} is attained by various approximator schemes, including those with one approximators (namely buw and p01). Such second and third lowest ε_{MS} are up to 100-fold larger than the lowest.

7.2 Sampling-based experimental results

Fig 3 depicts the experimental results of sampling-based approximation settings. They are from environments **h6** and **c10** with six and ten states, respectively. We evaluated two numbers of feature dimensions on every environment. This yields 4 subfigures: each is with two evaluation error metrics, namely ε_{PB} (total repb) and ε_{MS} (total rems), on the left and right vertical axes, respectively.

As can be observed, the magnitude ordering of the final ε_{PB} match with the exact results (hence, the theory). This is obvious from results on environment **h6**, where pinf attains the lowest final ε_{PB} , followed by paxmd, p02md, then p01 (the highest). We speculate that a similar pattern will emerge on the plot of environment **c10** as the number of experiment-episodes increases. That is, the error of pinf will keep decreasing until it crosses those of p02md then of paxmd (just as it crosses p01).

Such crossing occurs because the number of available samples per experiment-episode is inversely proportional to the number of anchors (approximators). In one extreme, each stepwise approximator of the pinf scheme receives only one sample per experiment-episode. On the other extreme, a single approximator of the p01 scheme receives as many samples as timesteps in an experiment-episode. This therefore results in p01 has lower ε_{PB} than pinf in the beginning, but then it plateaus at relatively high errors after some number of samples (the initial error decrease is not captured in the plot due to the coarse experiment-episode resolution in the horizontal axis). The ε_{PB} behaviours of p02md and paxmd are anticipated to be in between these two extremes.

On environments **h6** and **c10**, the progression and final values of ε_{MS} roughly follow those of ε_{PB} . Generally though, the rate of change of ε_{MS} is not as significant as ε_{PB} . A substantial drop in ε_{PB} may correspond to merely small drop in ε_{MS} , likewise with the increase. We can also observe less number of crossing in that ε_{MS} values of most schemes stay above or below the others: moving up, down or plateau together simultaneously.

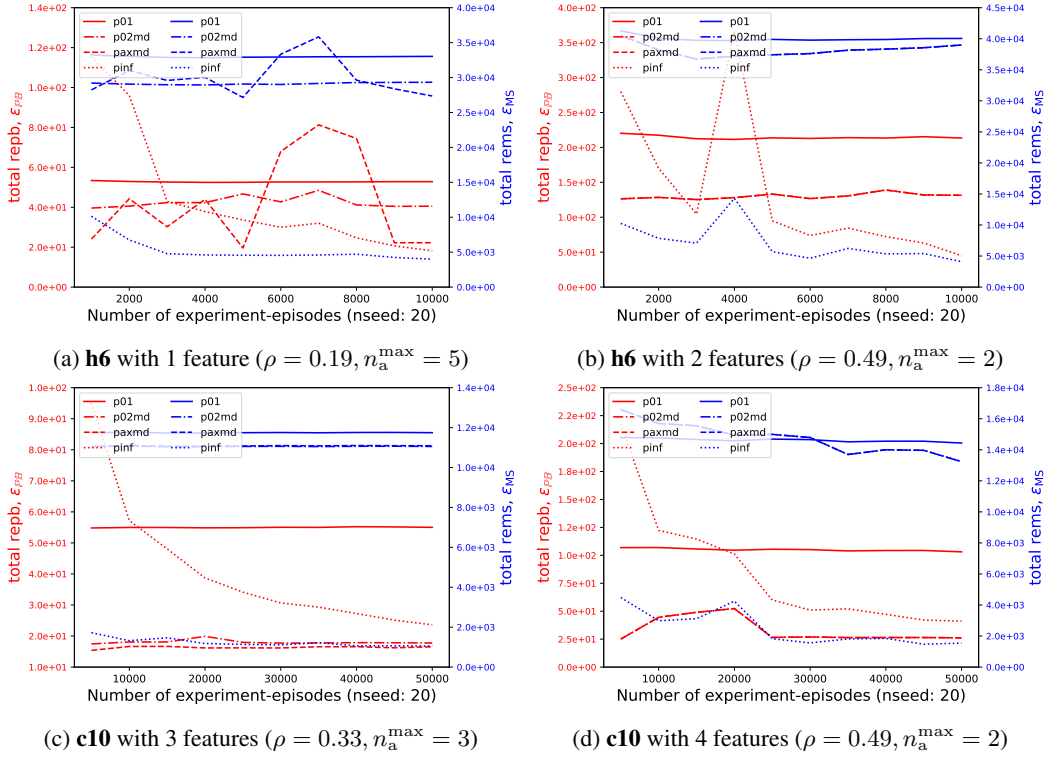


Figure 3: Sampling-based approximation results on environments **h6** (top row) and **c10** (bottom row). In each subplot, the **left red axis is ε_{PB} (total repb)**, whereas the **right blue axis is ε_{MS} (total rems)**, as in (30). Each line is interpolated from 10 data points, and averaged across 20 repetitions (20 different random-number-generator seeds). Note that the horizontal axes are different for **h6** and **c10**, where there are 10,000 and 50,000 total experiment-episodes (trials), respectively. The ticks in the vertical axes also vary across subplots.

Table 2: Non-sampling experimental results with feature-to-state dimensional ratio $\rho = 0.49$, allowing a maximum of $n_a^{\max} = 2$ anchors. The left most column contains environment identifiers (Sec 6.1), then the next ten columns contain ε_{PB} (total repb), whereas the last ten columns (gray highlighted) contain ε_{MS} (total rems), as in (30). For each evaluation metric, its ten columns represent ten schemes (Sec 6.3) with the following mnemonics: ‘buw’ is for the baseline unweighted scheme, ‘p’ is for the proposed general schemes whose variations are indicated by ‘02’, ‘ax’, or ‘inf’ for two anchors, the maximum number of anchors, or stepwise anchors, respectively, followed by ‘am’, ‘tv’, ‘ot’, or ‘md’ for the maximum absorption time, total variation, optimal transport, and MMD state distribution distance metrics, respectively. The red, green, and blue highlighted numbers indicate the lowest, the second lowest, and the third lowest error values in each 10-column group per row, respectively. We desire the lowest error (red). The NaN (Not a Number) indicates that $|\rho|S|$ yields either 0 feature dimension (hence, it cannot be implemented) or the same feature dimension as that of the lower ρ . In the latter case, the experiment is carried out only for the lower ρ (which induces a higher n_a^{\max}).

	total repb, ε_{PB}										total rems, ε_{MS}									
	buw	p01	p02am	p02tv	p02ot	p02md	paxtv	paxot	paxmd	pinf	buw	p01	p02am	p02tv	p02ot	p02md	paxtv	paxot	paxmd	pinf
h6	5.1e+03	2.1e+02	3.2e+02	4.8e+02	9.9e+01	1.3e+02	4.8e+02	9.9e+01	1.3e+02	2.8e-03	5.5e+04	4.0e+04	2.0e+03	4.2e+04	4.0e+04	4.0e+04	4.2e+04	4.0e+04	4.0e+04	1.1e+03
h36	8.2e+03	2.3e+02	2.0e+02	1.2e+02	1.3e+02	1.4e+02	1.2e+02	1.3e+02	1.4e+02	6.0e-02	1.2e+05	1.1e+05	1.4e+03	1.2e+05	4.1e+05	1.4e+05	1.2e+05	4.1e+05	1.4e+05	1.3e+03
h36c	1.3e+04	2.8e+02	2.4e+02	1.5e+02	2.1e+02	1.9e+02	1.5e+02	2.1e+02	1.9e+02	4.0e-02	1.9e+05	1.0e+05	2.1e+03	4.3e+05	6.4e+05	4.4e+05	4.3e+05	6.4e+05	4.4e+05	2.7e+03
h70	1.3e+04	3.8e+02	3.4e+02	2.4e+02	2.9e+02	3.2e+02	2.4e+02	2.9e+02	3.2e+02	1.1e+00	3.9e+05	2.0e+05	2.7e+03	2.3e+05	1.9e+05	5.5e+05	2.3e+05	1.9e+05	5.5e+05	2.6e+03
h100	1.9e+04	5.3e+02	4.9e+02	3.6e+02	3.4e+02	4.2e+02	3.6e+02	3.4e+02	4.2e+02	5.0e+00	7.4e+05	3.2e+05	4.7e+03	2.3e+05	3.7e+05	2.5e+05	2.3e+05	3.7e+05	2.5e+05	5.7e+03
c10	1.6e+04	2.9e+02	2.5e+02	1.2e+02	7.3e+01	5.7e+01	1.2e+02	7.3e+01	5.7e+01	7.4e-06	2.4e+05	1.6e+04	1.1e+03	1.6e+04	1.7e+04	1.7e+04	1.6e+04	1.7e+04	1.7e+04	3.2e+02
c35	1.8e+05	1.2e+02	7.0e+01	3.4e+01	3.9e+01	4.2e+01	3.4e+01	3.9e+01	4.2e+01	1.2e-02	4.1e+06	2.4e+04	4.0e+02	4.2e+04	4.6e+04	3.9e+04	4.2e+04	4.6e+04	3.9e+04	3.1e+02
c35c	1.3e+04	6.4e+01	4.6e+01	2.4e+01	2.8e+01	2.9e+01	2.4e+01	2.8e+01	2.9e+01	1.9e-02	2.6e+05	1.7e+04	3.5e+02	2.6e+04	2.9e+04	1.8e+05	2.6e+04	2.9e+04	1.8e+05	3.3e+02
c75	4.8e+03	1.7e+02	1.2e+02	7.2e+01	7.2e+01	8.5e+01	7.2e+01	7.2e+01	8.5e+01	1.8e-01	3.0e+05	5.5e+04	9.8e+02	1.2e+05	7.5e+04	9.8e+04	1.2e+05	7.5e+04	9.8e+04	8.2e+02
c100	4.9e+03	1.4e+02	1.2e+02	8.3e+01	7.7e+01	9.6e+01	8.3e+01	7.7e+01	9.6e+01	7.2e-01	4.0e+05	9.4e+04	1.3e+03	3.1e+05	1.3e+05	7.7e+04	3.1e+05	1.3e+05	7.7e+04	1.4e+03

Table 3: Non-sampling experimental results with $\rho = 0.33$, and $n_a^{\max} = 3$ anchors. For more descriptions, refer to the caption of Table 2.

	total repb, ε_{PB}										total rems, ε_{MS}									
	buw	p01	p02am	p02tv	p02ot	p02md	paxtv	paxot	paxmd	pinf	buw	p01	p02am	p02tv	p02ot	p02md	paxtv	paxot	paxmd	pinf
h6	NaN	NaN	NaN	NaN	NaN	NaN	NaN	NaN	NaN	NaN	NaN	NaN	NaN	NaN	NaN	NaN	NaN	NaN	NaN	NaN
h36	1.3e+04	4.5e+02	3.1e+02	1.5e+02	1.5e+02	1.8e+02	1.5e+02	1.2e+02	1.3e+02	2.5e-02	1.5e+05	9.0e+04	1.5e+03	1.5e+05	1.4e+05	2.7e+05	1.5e+05	1.4e+05	4.3e+05	1.4e+03
h36c	1.5e+04	3.1e+02	2.5e+02	1.6e+02	1.6e+02	1.6e+02	1.6e+02	1.4e+02	1.2e+02	9.1e-02	1.3e+05	8.0e+04	2.3e+03	1.7e+05	2.1e+05	1.7e+05	1.7e+05	1.6e+05	1.7e+05	2.5e+03
h70	1.7e+04	4.2e+02	3.5e+02	2.3e+02	2.5e+02	2.8e+02	2.3e+02	2.0e+02	2.0e+02	1.3e-01	4.8e+05	1.9e+05	2.8e+03	3.0e+05	2.5e+05	2.6e+05	3.0e+05	2.5e+05	2.4e+05	2.6e+03
h100	2.1e+04	5.6e+02	4.7e+02	3.5e+02	3.5e+02	4.0e+02	3.5e+02	3.2e+02	3.2e+02	1.5e+00	8.9e+05	3.1e+05	5.1e+03	9.5e+05	2.8e+05	3.4e+05	9.5e+05	3.2e+05	3.4e+05	4.6e+03
c10	9.1e+02	9.4e+01	6.0e+01	3.0e+01	2.0e+01	2.7e+01	3.0e+01	2.3e+01	2.5e+01	6.5e-09	1.4e+04	1.2e+04	2.0e+03	1.1e+04	1.1e+04	1.1e+04	1.1e+04	1.1e+04	1.1e+04	1.9e+03
c35	4.0e+03	2.4e+02	9.3e+01	5.1e+01	4.9e+01	6.0e+01	5.1e+01	4.0e+01	4.4e+01	1.5e-01	1.1e+05	3.1e+04	4.9e+02	3.3e+04	4.5e+04	1.1e+05	3.3e+04	5.2e+04	4.3e+04	3.4e+02
c35c	2.1e+03	1.1e+02	5.8e+01	3.9e+01	4.0e+01	3.3e+01	3.9e+01	4.2e+01	2.5e+01	3.3e-01	2.9e+04	2.0e+04	4.1e+02	3.9e+04	5.4e+04	3.7e+04	3.9e+04	6.0e+04	2.9e+04	7.4e+02
c75	4.3e+03	2.6e+02	1.4e+02	6.6e+01	7.6e+01	8.7e+01	6.6e+01	6.0e+01	6.4e+01	3.7e-02	3.5e+05	6.0e+04	1.1e+03	6.5e+04	7.2e+04	1.5e+05	6.5e+04	5.9e+04	7.1e+04	8.2e+02
c100	4.4e+03	1.7e+02	1.2e+02	7.3e+01	7.9e+01	1.1e+02	7.3e+01	7.4e+01	6.9e+01	5.7e-02	4.7e+05	8.8e+04	1.4e+03	9.1e+04	7.2e+04	3.6e+05	9.1e+04	7.8e+04	8.5e+04	1.2e+03

Table 4: Non-sampling experimental results with $\rho = 0.19$, and $n_a^{\max} = 5$ anchors. For more descriptions, refer to the caption of Table 2.

	total repb, ε_{PB}										total rems, ε_{MS}									
	buw	p01	p02am	p02tv	p02ot	p02md	paxtv	paxot	paxmd	pinf	buw	p01	p02am	p02tv	p02ot	p02md	paxtv	paxot	paxmd	pinf
h6	1.5e+03	5.3e+01	1.2e+02	1.5e+02	1.3e+02	4.2e+01	9.7e+01	2.6e+01	2.7e+01	2.3e-14	1.0e+05	3.3e+04	4.6e+03	3.7e+04	3.6e+04	3.0e+04	3.6e+04	3.1e+04	3.1e+04	4.8e+03
h36	1.7e+04	1.1e+03	4.7e+02	2.0e+02	2.6e+02	2.5e+02	1.1e+02	1.0e+02	8.6e+01	9.8e-02	1.7e+05	1.4e+05	2.0e+03	1.8e+05	1.9e+05	2.7e+05	6.8e+05	3.8e+05	2.2e+05	1.6e+03
h36c	1.2e+04	4.4e+02	2.3e+02	1.1e+02	1.2e+02	1.2e+02	7.0e+01	5.3e+01	5.2e+01	7.0e-01	9.7e+04	5.7e+04	2.4e+03	8.0e+04	8.6e+04	8.1e+04	4.0e+05	8.5e+04	8.2e+04	2.2e+03
h70	2.1e+04	5.9e+02	3.9e+02	2.4e+02	2.5e+02	2.9e+02	1.8e+02	1.6e+02	1.3e+02	4.3e-01	5.5e+05	1.8e+05	3.0e+03	2.1e+05	1.9e+05	2.3e+05	9.0e+05	1.7e+06	5.9e+05	2.6e+03
h100	2.6e+04	7.0e+02	5.0e+02	3.2e+02	3.5e+02	3.8e+02	2.3e+02	2.2e+02	1.9e+02	1.1e-01	1.1e+06	2.9e+05	5.2e+03	4.0e+05	2.9e+05	3.0e+05	4.3e+05	6.1e+05	5.5e+05	4.8e+03
c10	2.4e+02	8.3e+00	1.1e+01	8.7e+00	8.8e+00	7.2e+00	3.4e+00	2.6e+00	2.8e+00	6.1e-14	2.2e+04	8.8e+03	3.0e+03	8.9e+03	9.0e+03	8.8e+03	9.4e+03	8.8e+03	9.0e+03	3.2e+03
c35	4.4e+03	8.5e+03	1.1e+02	5.2e+02	4.7e+02	4.5e+02	2.6e+02	1.7e+02	2.0e+02	6.0e-02	1.3e+05	1.5e+06	6.7e+02	1.8e+05	1.8e+05	1.8e+05	1.5e+05	4.3e+04	2.1e+05	4.8e+02
c35c	2.2e+03	7.3e+02	7.8e+01	3.0e+02	7.3e+01	2.1e+02	1.4e+02	1.3e+02	1.6e+02	5.7e-02	3.6e+04	6.7e+04	5.1e+02	7.4e+04	7.2e+04	7.6e+04	8.4e+04	9.7e+04	8.2e+04	4.0e+02
c75	4.3e+03	4.2e+02	1.5e+02	9.6e+01	1.0e+02	7.9e+01	5.1e+01	4.6e+01	6.8e+01	6.7e-02	4.1e+05	6.7e+04	1.2e+03	7.2e+04	9.8e+04	7.8e+04	8.4e+04	9.3e+04	2.6e+05	9.3e+02
c100	4.3e+03	2.2e+02	1.1e+02	7.3e+01	7.8e+01	7.3e+01	4.3e+01	4.7e+01	3.8e+01	9.8e-02	5.8e+05	8.6e+04	1.5e+03	8.0e+04	7.2e+04	8.4e+04	1.2e+05	2.0e+05	1.1e+05	1.3e+03

Table 5: Non-sampling experimental results with $\rho = 0.09$, and $n_a^{\max} = 11$ anchors. For more descriptions, refer to the caption of Table 2.

	total repb, ε_{PB}										total rems, ε_{MS}									
	buw	p01	p02am	p02tv	p02ot	p02md	paxtv	paxot	paxmd	pinf	buw	p01	p02am	p02tv	p02ot	p02md	paxtv	paxot	paxmd	pinf
h6	NaN	NaN	NaN	NaN	NaN	NaN	NaN	NaN	NaN	NaN	NaN	NaN	NaN	NaN	NaN	NaN	NaN	NaN	NaN	NaN
h36	1.8e+04	5.6e+04	7.1e+02	5.7e+03	3.8e+03	7.4e+02	4.4e+02	3.6e+02	2.2e+02	1.9e-02	2.2e+05	4.9e+06	3.1e+03	2.0e+06	1.1e+06	5.2e+05	4.2e+05	5.1e+05	4.4e+05	2.4e+03
h36c	7.8e+03	3.3e+03	2.4e+02	1.3e+03	1.5e+03	1.8e+03	5.2e+02	2.1e+02	4.1e+02	2.7e-02	8.2e+04	2.2e+05	2.6e+03	2.9e+05	2.2e+05	9.5e+05	8.2e+05	5.2e+05	6.0e+05	2.5e+03
h70	2.7e+04	1.8e+03	7.0e+02	3.5e+02	3.6e+02	4.2e+02	1.0e+02	8.5e+01	1.9e+02	5.7e-02	6.2e+05	1.4e+05	3.8e+03	2.4e+05	2.2e+05	3.0e+05	3.5e+05	3.2e+05	5.4e+06	3.1e+03
h100	3.1e+04	1.4e+03	6.8e+02	4.0e+02	5.0e+02	8.2e+02	1.3e+02	1.2e+02	9.6e+01	7.9e-02	1.1e+06	3.2e+05	5.9e+03	3.6e+05	3.2e+05	9.7e+06	5.2e+05	4.8e+05	4.5e+05	5.1e+03
c10	NaN	NaN	NaN	NaN	NaN	NaN	NaN	NaN	NaN	NaN	NaN	NaN	NaN	NaN	NaN	NaN	NaN	NaN	NaN	NaN
c35	2.7e+03	7.4e+02	7.7e+01	1.8e+02	1.4e+02	8.9e+01	2.7e+02	3.5e+01	1.4e+01	1.0e-06	1.3e+05	3.2e+05	4.3e+03	4.4e+05	2.6e+05	3.2e+05	1.5e+05	1.1e+05	1.0e+05	4.5e+03
c35c	1.2e+03	5.7e+02	4.1e+01	1.2e+02	6.6e+01	2.9e+01	4.5e+01	1.7e+01	1.5e+01	3.8e-07	3.4e+04	4.8e+05	2.6e+03	2.2e+05	1.6e+05	1.5e+05	1.8e+05	1.4e+05	1.4e+05	2.9e+03
c75	4.6e+03	2.1e+03	1.7e+02	8.5e+02	7.7e+02	5.2e+02	1.6e+02	9.3e+03	7.7e+01	2.3e-01	4.4e+05	1.8e+05	1.4e+03	2.9e+05	2.6e+05	2.1e+05	3.5e+05	3.9e+06	2.8e+05	1.4e+03
c100	4.9e+03	4.9e+02	1.2e+02	1.4e+02	1.7e+02	7.9e+01	2.3e+01	2.9e+02	2.8e+02	8.4e-02	6.1e+05	8.7e+04	1.5e+03	7.8e+04	7.3e+04	9.5e+04	3.0e+05	2.3e+07	4.2e+06	1.4e+03

Table 6: Non-sampling experimental results with $\rho = 0.06$, and $n_a^{\max} = 16$ anchors. For more descriptions, refer to the caption of Table 2.

	total repb, ε_{PB}											total rems, ε_{MS}										
	buw	p01	p02am	p02tv	p02ot	p02md	paxtv	paxot	paxmd	pinf	buw	p01	p02am	p02tv	p02ot	p02md	paxtv	paxot	paxmd	pinf		
h6	NaN	NaN	NaN	NaN	NaN	NaN	NaN	NaN	NaN	NaN	NaN	NaN	NaN	NaN	NaN	NaN	NaN	NaN	NaN	NaN		
h36	1.1e+04	1.8e+03	3.9e+02	2.4e+02	5.1e+02	2.2e+02	5.0e+01	7.3e+01	3.4e+01	4.6e-01	2.6e+05	1.6e+06	4.9e+03	1.5e+06	4.4e+06	7.8e+05	6.5e+05	7.2e+05	2.2e+06	5.1e+03		
h36c	5.1e+03	1.2e+03	1.4e+02	1.3e+02	1.2e+03	1.4e+02	1.4e+01	4.2e+01	1.5e+01	9.6e-02	7.2e+04	8.4e+05	2.9e+03	5.2e+05	3.0e+06	1.2e+06	2.1e+06	3.8e+05	3.1e+05	8.3e+03		
h70	2.9e+04	7.1e+03	1.1e+03	1.2e+03	1.1e+03	5.9e+02	9.9e+01	1.3e+02	1.4e+02	4.8e-01	6.3e+05	3.8e+05	5.5e+03	4.4e+05	4.7e+05	4.3e+05	5.2e+05	7.5e+05	9.8e+05	4.0e+03		
h100	3.2e+04	2.3e+03	8.0e+02	4.7e+02	5.8e+02	5.4e+02	7.2e+01	7.9e+01	7.6e+01	3.1e-01	1.2e+06	3.1e+05	6.2e+03	3.4e+05	2.7e+05	6.9e+05	6.3e+05	4.0e+05	5.5e+05	5.3e+03		
c10	NaN	NaN	NaN	NaN	NaN	NaN	NaN	NaN	NaN	NaN	NaN	NaN	NaN	NaN	NaN	NaN	NaN	NaN	NaN	NaN		
c35	4.2e+03	3.3e+02	6.0e+01	3.5e+01	3.1e+01	2.4e+01	4.7e+00	8.0e+00	9.1e+00	3.2e-07	2.3e+05	5.1e+05	6.3e+03	1.3e+05	1.1e+05	8.4e+04	8.0e+04	8.9e+04	7.3e+04	8.0e+03		
c35c	8.2e+02	2.5e+02	2.2e+01	3.4e+01	1.3e+01	1.4e+01	3.9e+00	7.6e+00	4.9e+00	4.6e-10	3.7e+04	3.7e+05	3.8e+03	1.1e+05	9.1e+04	9.1e+04	7.3e+04	8.7e+04	8.9e+04	4.0e+03		
c75	4.1e+03	1.9e+03	1.3e+02	5.4e+03	5.8e+02	2.4e+02	2.5e+01	1.2e+02	9.3e+01	1.8e-03	4.4e+05	5.4e+05	1.4e+03	3.6e+07	1.9e+06	1.1e+06	6.0e+05	7.4e+05	1.5e+06	1.6e+03		
c100	5.3e+03	1.3e+03	1.4e+02	5.3e+02	5.0e+02	1.4e+02	3.6e+01	4.2e+01	2.6e+01	1.3e-01	6.3e+05	1.1e+05	1.6e+03	1.1e+05	1.1e+05	1.4e+05	1.7e+05	1.3e+05	1.4e+05	1.4e+03		

25

Table 7: Non-sampling experimental results with $\rho = 0.03$, and $n_a^{\max} = 33$ anchors. For more descriptions, refer to the caption of Table 2.

	total repb, ε_{PB}											total rems, ε_{MS}										
	buw	p01	p02am	p02tv	p02ot	p02md	paxtv	paxot	paxmd	pinf	buw	p01	p02am	p02tv	p02ot	p02md	paxtv	paxot	paxmd	pinf		
h6	NaN	NaN	NaN	NaN	NaN	NaN	NaN	NaN	NaN	NaN	NaN	NaN	NaN	NaN	NaN	NaN	NaN	NaN	NaN	NaN		
h36	8.4e+02	1.2e+03	2.0e+02	8.3e+01	9.6e+01	7.4e+01	1.7e+01	1.6e+01	1.6e+01	1.3e-12	3.3e+05	2.5e+06	2.1e+04	1.1e+06	1.0e+06	9.4e+05	5.9e+05	6.0e+05	6.0e+05	1.6e+04		
h36c	2.2e+02	3.0e+02	4.8e+01	4.9e+01	9.8e+02	2.9e+01	1.7e+00	1.8e+00	2.2e+00	2.3e-13	7.9e+04	4.8e+05	8.6e+03	4.2e+05	8.0e+06	3.2e+05	2.3e+05	2.4e+05	2.4e+05	8.2e+03		
h70	1.4e+04	4.4e+03	4.6e+02	4.2e+02	3.6e+02	3.3e+02	2.0e+01	3.3e+01	4.1e+01	1.1e-04	5.8e+05	5.5e+06	6.4e+03	3.5e+06	3.5e+06	4.3e+06	1.8e+06	2.1e+06	1.7e+06	1.1e+04		
h100	4.2e+04	2.6e+04	4.1e+03	7.0e+03	7.3e+03	1.0e+04	8.3e+02	3.9e+02	7.2e+02	3.7e+00	1.1e+06	1.6e+06	1.4e+04	1.8e+06	1.5e+06	2.4e+06	1.0e+06	1.3e+06	1.4e+06	7.2e+03		
c10	NaN	NaN	NaN	NaN	NaN	NaN	NaN	NaN	NaN	NaN	NaN	NaN	NaN	NaN	NaN	NaN	NaN	NaN	NaN	NaN		
c35	6.5e+02	9.1e+01	2.4e+01	9.4e+00	8.5e+00	6.1e+00	1.7e+00	2.0e+00	2.7e+00	4.0e-13	4.2e+05	2.6e+05	8.4e+03	1.0e+05	9.3e+04	7.6e+04	6.9e+04	6.2e+04	6.2e+04	8.0e+03		
c35c	6.5e+01	6.0e+01	2.1e+01	8.7e+00	4.0e+00	5.0e+00	1.3e+00	1.1e+00	1.2e+00	6.2e-13	3.6e+04	1.3e+05	5.2e+03	7.1e+04	6.3e+04	6.6e+04	6.3e+04	4.5e+04	6.3e+04	5.1e+03		
c75	2.1e+03	4.0e+03	5.6e+01	4.0e+02	9.2e+01	3.6e+01	3.5e+00	8.6e+00	3.5e+00	7.0e-09	4.3e+05	1.5e+07	1.1e+04	7.1e+06	7.7e+05	2.2e+05	1.6e+05	2.4e+05	1.6e+05	1.2e+04		
c100	3.8e+03	6.2e+04	1.2e+02	3.6e+02	2.1e+02	1.2e+02	9.5e+00	2.5e+01	1.4e+01	2.3e-05	6.7e+05	6.7e+07	4.8e+03	8.1e+05	5.9e+05	5.0e+05	3.0e+05	1.2e+06	3.3e+05	5.0e+03		

8 Conclusions, limitations, and future works

We propose a system of seminorm LSTD approximators for estimating the relative bias value from multiple transient and multiple recurrent states in unichain MDPs. To this end, we derive an expression for the minimizer of the seminorm LSTD that enables approximation through sampling (as for model-free RL). We also devise a general procedure for LSTD-based policy evaluation, from which the relative value approximator emerges as a special case; so do the other existing LSTD-based approximators for recurrent MDPs and unichain MDPs with one 0-reward recurrent state. Experimental results validate that a system with more approximators yields the lower projected Bellman errors. It is also empirically shown that timestep-neighborhoods can reasonably be specified based on estimating the squared MMD among stepwise state distributions (using their state samples).

The proposed method addresses the problem of minimizing MSBPE that is based on the one-step Bellman operator \mathbb{B} in (3). It is known that \mathbb{B} can be extended to its multi-step variant. That is,

$$\mathbf{v} = \mathbb{B}^m[\mathbf{v}] := \left\{ \sum_{\tau=0}^{m-1} \mathbf{P}^\tau (\mathbf{r} - \mathbf{g}) \right\} + \mathbf{P}^m \mathbf{v}, \quad \text{for } m \geq 1 \text{ (where } m = 1 \text{ gives the one-step variant).}$$

Another known extension is to utilize a weighted average over all \mathbb{B}^m for $m = 1, 2, \dots$, which gives

$$\mathbf{v} = \mathbb{B}_\lambda[\mathbf{v}], \quad \text{where } \mathbb{B}_\lambda := (1 - \lambda) \sum_{m=1}^{\infty} \lambda^{m-1} \mathbb{B}^m, \text{ for a trace-decay factor } \lambda \in [0, 1).$$

These two extensions essentially provide a way to control the bias-variance trade-off in the value approximation.¹⁰ They lead to m -step TD, TD(λ) and LSTD(λ) algorithms (Sutton, 1988; Boyan, 2002). It is interesting therefore to extend our proposed method to a system of multiple m -step seminorm LSTD (or seminorm LSTD(λ)) approximators. This includes examination about how the size of a neighborhood affects the suitable values for m and λ .

This work has not taken the advantage of iterative techniques for calculating the Moore-Penrose pseudoinverse (for computing the minimizer of the seminorm LSTD). It also has not exploited the fact that $(1, 3)$ -pseudoinverse is sufficient for an LS solution that is not necessarily a minimum-norm solution (Campbell and Meyer, 2009, Table 6.1). Note that the pseudoinverse used throughout this work, i.e. M^\dagger for a matrix M , is the full $(1, 2, 3, 4)$ -pseudoinverse.

Additionally, the (finite) sample complexity of the proposed method deserves a careful study. This includes the relationship between the number of neighborhoods and the number of samples to achieve a certain level of errors. We anticipate an intricate interplay because a fewer number of neighborhoods (equivalently, more neighbors per neighborhood) yields more violation to the i.i.d sample condition in computing the sample means for the minimizing parameter of the seminorm LSTD (Thm 3.1).

Lastly, our proposed method can be modified to become a system of semi-gradient seminorm TD approximators. This is worth investigating because semi-gradient algorithms involve an initial parameter value, which is paradoxically beneficial for policy iteration RL methods in that it can be set to the parameter of the last policy's value approximator. The modification should leverage the fact that both semi-gradient TD and LSTD algorithms converge to the same TD fixed point (Sec 2).

¹⁰One way to see this bias-variance trade-off is from the semi-gradient TD viewpoint as follows. Setting m to 1 leads to the one-step TD algorithm. As in (12), it approximates the true value $v(s_t) \approx r_{t+1} - g + \hat{v}(s_{t+1})$, which has low variance (as it involves only one-step next state and reward samples) but is biased towards the estimator \hat{v} . On the other hand, m -step TD with m approaches infinity approximates $v(s_t) \approx (r_{t+1} - g) + (r_{t+2} - g) + \dots$, which is unbiased (due to no involvement of \hat{v}) but has high variance (due to an infinitely long sequence of reward samples). Note that in practice, the gain g should also be approximated.

References

- Ben-Israel, A. and Greville, T. (2003). *Generalized Inverses: Theory and Applications*. CMS Books in Mathematics. Springer. (page 5)
- Boyan, J. A. (2002). Technical update: Least-squares temporal difference learning. *Machine Learning*, 49. (pages 10 and 26)
- Bradtke, S. J. and Barto, A. G. (1996). Linear least-squares algorithms for temporal difference learning. *Machine Learning*, 22(1–3). (pages 2, 10, and 19)
- Campbell, S. L. and Meyer, C. D. (2009). *Generalized Inverses of Linear Transformations*. Society for Industrial and Applied Mathematics. (pages 5, 7, 8, and 26)
- Castro, P. S. (2020). Scalable methods for computing state similarity in deterministic Markov decision processes. *Proceedings of the AAAI Conference on Artificial Intelligence*. (page 19)
- Dann, C., Neumann, G., and Peters, J. (2014). Policy evaluation with temporal differences: A survey and comparison. *Journal of Machine Learning Research*, 15(24). (pages 2, 8, and 21)
- Ferns, N., Castro, P. S., Precup, D., and Panangaden, P. (2006). Methods for computing state similarity in Markov decision processes. In *Conference in Uncertainty in Artificial Intelligence*. (page 13)
- Flamary, R., Courty, N., Gramfort, A., Alaya, M. Z., Boisbunon, A., Chambon, S., Chapel, L., Corenflos, A., Fatras, K., Fournier, N., Gautheron, L., Gayraud, N. T., Janati, H., Rakotomamonjy, A., Redko, I., Rolet, A., Schutz, A., Seguy, V., Sutherland, D. J., Tavenard, R., Tong, A., and Vayer, T. (2021). POT: Python optimal transport. *Journal of Machine Learning Research*, 22(78). (page 19)
- Gretton, A., Borgwardt, K. M., Rasch, M. J., Schölkopf, B., and Smola, A. (2012). A kernel two-sample test. *Journal of Machine Learning Research*, 13(25). (pages 12 and 13)
- Grinstead, C. and Snell, J. (2012). *Introduction to Probability*. American Mathematical Society. (page 11)
- Grünewälder, S., Lever, G., Baldassarre, L., Pontil, M., and Gretton, A. (2012). Modelling transition dynamics in MDPs with RKHS embeddings. In *Proceedings of the 29th International Conference on Machine Learning*. (page 13)
- Haasdonk, B. and Bahlmann, C. (2004). Learning with distance substitution kernels. In *Pattern Recognition*, volume 3175. Springer Berlin Heidelberg. (page 13)
- Hartwig, R. (1986). The reverse order law revisited. *Linear Algebra and its Applications*, 76. (page 7)
- Harville, D. A. (1997). *Matrix Algebra From a Statistician's Perspective*. Springer. (page 6)
- Hordijk, A., Dekker, R., and Kallenberg, L. C. M. (1985). Sensitivity analysis in discounted Markovian decision problems. *Operations Research Spektrum*, 7. (page 16)
- Lan, C. L., Bellemare, M. G., and Castro, P. S. (2021). Metrics and continuity in reinforcement learning. In *Proceedings of the AAAI Conference on Artificial Intelligence*. (page 19)
- Lewis, T. O. and Newman, T. G. (1968). Pseudoinverses of positive semidefinite matrices. *SIAM Journal on Applied Mathematics*, 16(4). (page 6)
- Liu, R. and Olshevsky, A. (2021). Temporal difference learning as gradient splitting. In *Proceedings of the 38th International Conference on Machine Learning*. (page 2)
- Muandet, K., Fukumizu, K., Sriperumbudur, B., and Schölkopf, B. (2017). Kernel mean embedding of distributions: A review and beyond. *Foundations and Trends® in Machine Learning*, 10. (page 13)
- Proszynski, W. and Sosnowski, A. (1995). Matrix expressions for minimum seminorm least squares solutions of linear systems and the related inverse. *Demonstratio Mathematica*, 28(3). (page 6)

- Puterman, M. L. (1994). *Markov Decision Processes: Discrete Stochastic Dynamic Programming*. John Wiley & Sons, Inc., 1st edition. (pages 4 and 14)
- Song, T., Li, D., Cao, L., and Hirasawa, K. (2016). Kernel-based least squares temporal difference with gradient correction. *IEEE Transactions on Neural Networks and Learning Systems*, 27(4). (page 13)
- Strens, M. J. A. (2000). A Bayesian framework for reinforcement learning. In *Proceedings of the 27th International Conference on Machine Learning*. (page 16)
- Sugiyama, M., Suzuki, T., and Kanamori, T. (2012). *Density Ratio Estimation in Machine Learning*. Cambridge University Press. (page 12)
- Sutton, R. S. (1988). Learning to predict by the methods of temporal differences. *Machine Learning*, 3(1). (page 26)
- Sutton, R. S. and Barto, A. G. (2018). *Introduction to Reinforcement Learning*. MIT Press. (pages 4 and 7)
- Tian, Y. (2019). Reverse order laws for generalized inverses of products of two or three matrices with applications. *arXiv:1912.05948*. (page 7)
- Tsitsiklis, J. N. and Roy, B. V. (1999). Average cost temporal-difference learning. *Automatica*, 35(11). (page 4)
- Ueno, T., Kawanabe, M., Mori, T., Maeda, S.-i., and Ishii, S. (2008). A semiparametric statistical approach to model-free policy evaluation. In *Proceedings of the 25th International Conference on Machine Learning*. (page 10)
- Xu, X., Xie, T., Hu, D., and Lu, X. (2005). Kernel least-squares temporal difference learning. *Information Technology - IT*, 11. (page 13)
- Yu, H. and Bertsekas, D. P. (2009). Convergence results for some temporal difference methods based on least squares. *IEEE Transactions on Automatic Control*, 54(7). (pages 4, 9, 10, and 19)